Supporting Information

Using Unnatural Amino Acids to Probe the Energetics of Oxyanion Hole Hydrogen Bonds in the Ketosteroid Isomerase Active Site

Aditya Natarajan, Jason P. Schwans, Daniel Herschlag

Supporting Text

I. Active site titrations of semisynthetic enzymes

Semisynthetic Tyr, 2-F-Tyr, 3-F-Tyr, 2,6-F_2-Tyr, and 3-Cl-Tyr substituted KSI variants with a D40N mutation were prepared, with the additional mutations made to the KSI amino acid sequence to facilitate semisynthesis as described in the main text. The D40N mutation was also inserted to enable tight binding to and thus active site titration with the inhibitor equilenin.[1]

We first determined the affinity of KSI variants for a fluorescent analog of equilenin, EqA488-1, which contains an Alexa-488 dye covalently linked to the C17 position on the D ring of equilenin, as previously described (Figure S9, Table S6).[1] Previous experiments showed that the fluorescence of EqA488-1 is quenched upon addition of KSI and that the dissociation constant obtained using EqA488-1 is the same as that obtained for unmodified equilenin.[1] The higher intrinsic fluorescence of EqA488-1 relative to equilenin enabled the use of sub-nanomolar concentrations of EqA488-1, well below the K_d, and thereby more precise affinity determinations.

We then performed active site titrations with the concentration of equilenin held constant and >100-fold greater than the K_d for EqA488-1 determined above. We monitored equilenin fluorescence over a range of enzyme concentrations that varied from well below to up to twice the total concentration of equilenin (Figure S10). We used equilenin instead of EqA488-1 for

these titrations, as these experiments required the use of high ligand concentrations (900 nM) at which the intrinsic fluorescence of equilenin is high enough to be precisely determined. As expected under these conditions, equilenin fluorescence decreased nearly linearly with increasing enzyme concentration at sub-stoichiometric levels of enzyme, and showed little or no change at super-stoichiometric enzyme concentrations (Figure S10). The fraction of enzyme that could bind equilenin was determined from fits of these data to a quadratic binding isotherm (Equation 3 in Experimental Procedures), with the affinity for equilenin fixed to the values determined independently (Table S6). As expected, one equivalent of expressed KSI could saturate one equivalent of equilenin (Table S7). The fraction of semisynthetic enzymes determined that could bind equilenin ranged from 0.75 to 1.18, consistent with all or nearly all of each semisynthetic enzyme being in a fully active conformation (Table S7).

II. Generating 4,4-dideuterated 5(10)-EST for kinetic isotope effect determinations

We generated 4,4-dideuterated (^{2}H) 5(10)-EST as follows. Many dienolate ions are protonated more rapidly on the α-carbon than on the γ-carbon in aqueous solution, thereby generating β,γ-unsaturated instead of α,β-unsaturated enones.[2-5] For KSI, this corresponds to generation of substrate rather than product (Figure 1). Monitoring the reaction of protiated (^{1}H) 5(10)-EST with 1 mM sodium deuteroxide (NaOD) in 9:1 CD_3OD:D_2O by ^{1}H NMR, we observed the disappearance of peaks at 2.72 and 2.84 ppm corresponding to the α-hydrogen atoms in 5(10)-EST with a half-life of ~1-2 minutes, and no peaks at 2.2 – 2.4 ppm that presumably correspond to the γ-hydrogen atoms on the B ring in the conjugated product 4-EST after 18 minutes (Figure S11) (The γ-hydrogen atoms on the B ring are not expected to undergo H/D exchange under these conditions, based on a previously determined rate constant of 2×10^{-3} M^{-1} s^{-1} for deuteroxide-mediated H/D exchange at this position in the structurally similar product 4-androstene-3,17-dione.[5]). These observations are consistent with nearly complete H/D exchange at the α-carbon (~95%) with little or no concomitant product (4-EST) formation (<2%) over this timescale.

Adding protiated 5(10)-EST to deuterated buffer (≥99 atom %D) containing KSI results in biphasic product formation, with the first phase likely arising from reaction of protiated 5(10)-EST and the second phase presumably originating from reaction of deuterated 5(10)-EST generated via substrate reformation from the intermediate after H/D exchange of protonated general base with solvent. In contrast, 4,4-dideuterated 5(10)-EST, generated with low concentrations of NaOD in D_2O as above and diluted to subsaturating final concentrations into deuterated buffer containing KSI, resulted in single exponential product formation with rate

constants that increased linearly with enzyme concentration, that were ~7-fold lower than those observed with protiated 5(10)-EST (Figure S12A-C), and these rate contants were the same, within error, as the second phase of the reactions of protiated 5(10)-EST in D_2O (not shown). The rate constants obtained upon adding substrate that had been incubated with either H_2O alone or 1 mM NaOH in H_2O for 18 minutes agreed within 3% (Figure S12D), further indicating that incubating substrate with strong base did not result in the formation of side products that inhibited or otherwise perturbed the enzymatic reaction.

References

(1) Kraut, D. A.; Sigala, P. A.; Pybus, B.; Liu, C. W.; Ringe, D.; Petsko, G. A.; Herschlag, D. *PLoS Biol.* **2006**, *4*, 501–519.
(2) Ringold, H. J.; Malhotra, S. K. *Tetrahedron Lett* **1962**, *3*, 669–672.
(3) Whalen, D. L.; Weimaster, J. F.; Ross, A. M.; Radhe, R. *J. Am. Chem. Soc.* **1976**, *98*, 7319–7324.
(4) Perera, S. K.; Dunn, W. A.; Fedor, L. R. *J. Org. Chem.* **1980**, *45*, 2816–2821.
(5) Pollack, R. M.; Zeng, B.; Mack, J. P.; Eldin, S. *J. Am. Chem. Soc.* **1989**, *111*, 6419–6423.
(6) Schwans, J. P.; Sunden, F.; Gonzalez, A.; Tsai, Y.; Herschlag, D. *J. Am. Chem. Soc.* **2011**, *133*, 20052–20055
(7) Schwans, J. P.; Kraut, D. A.; Herschlag, D. *Proc. Natl. Acad. Sci. USA* **2009**, *106*, 14271-14275

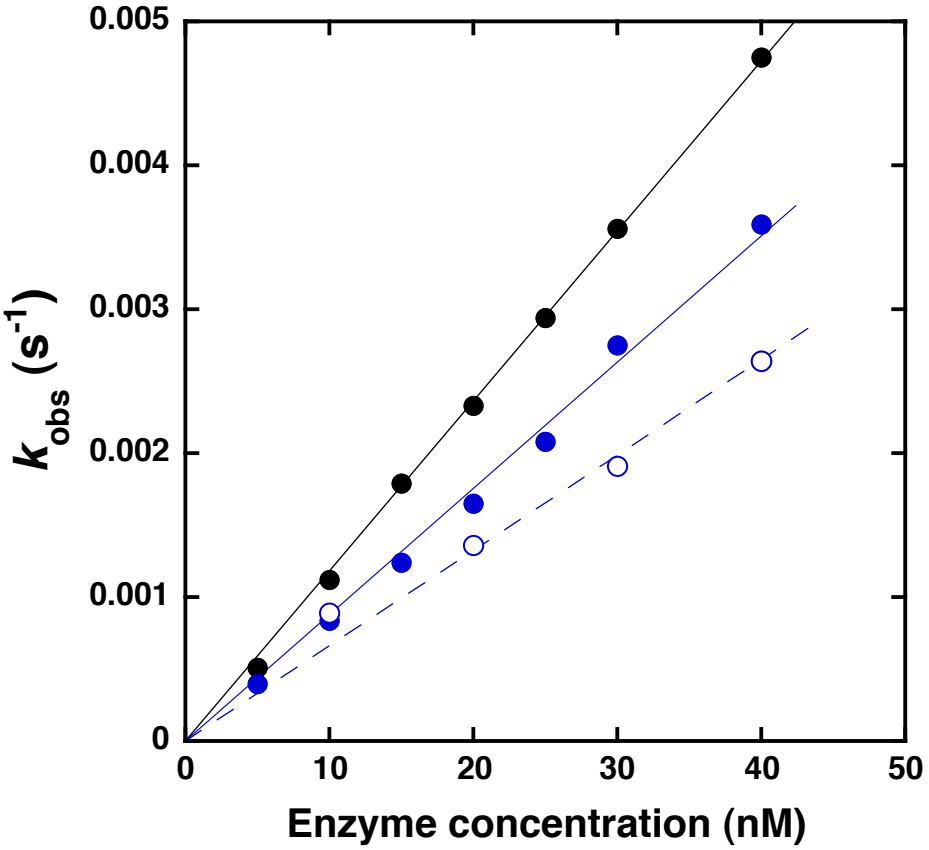

Figure S1. Activity of recombinant (black) and semisynthetic (blue) WT KSI with subsaturating 5(10)-EST (4.7 μM). Kinetic parameters for independent preparations of semisynthetic WT KSI are shown as open and closed blue circles. The values of k_{cat}/K_M from the fits shown are: 11.8 × 10^4 M^{-1} s^{-1} (recombinant), 8.8 × 10^4 M^{-1} s^{-1} (semisynthetic, closed circles), 6.8 × 10^4 M^{-1} s^{-1} (semisynthetic, open circles). Conditions: 40 mM potassium phosphate, 1 mM EDTA, 2% DMSO (v/v), pH 7.2.

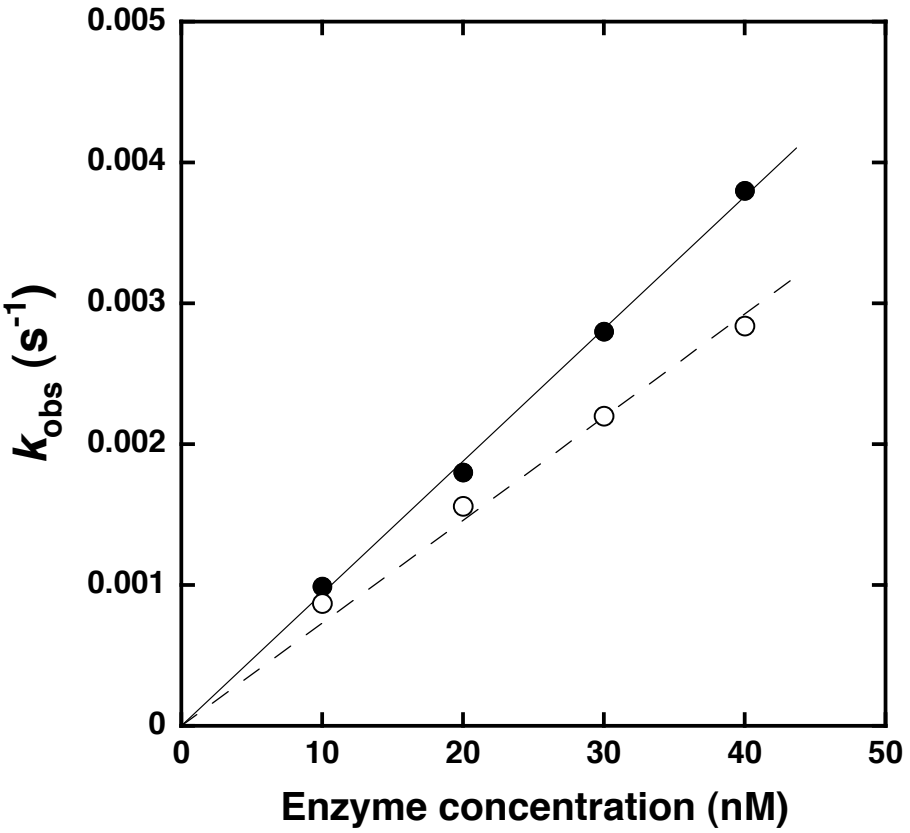

Figure S2. Activity of independent preparations (open and closed symbols) of semisynthetic 2-F-Tyr KSI with subsaturating 5(10)-EST (4.7 μM). The values of k_{cat}/K_M from the fits shown are: 9.4×10^4 M^{-1} s^{-1} (closed circles), 7.3×10^4 M^{-1} s^{-1} (open circles). Conditions: 40 mM potassium phosphate, 1 mM EDTA, 2% DMSO (v/v), pH 7.2.

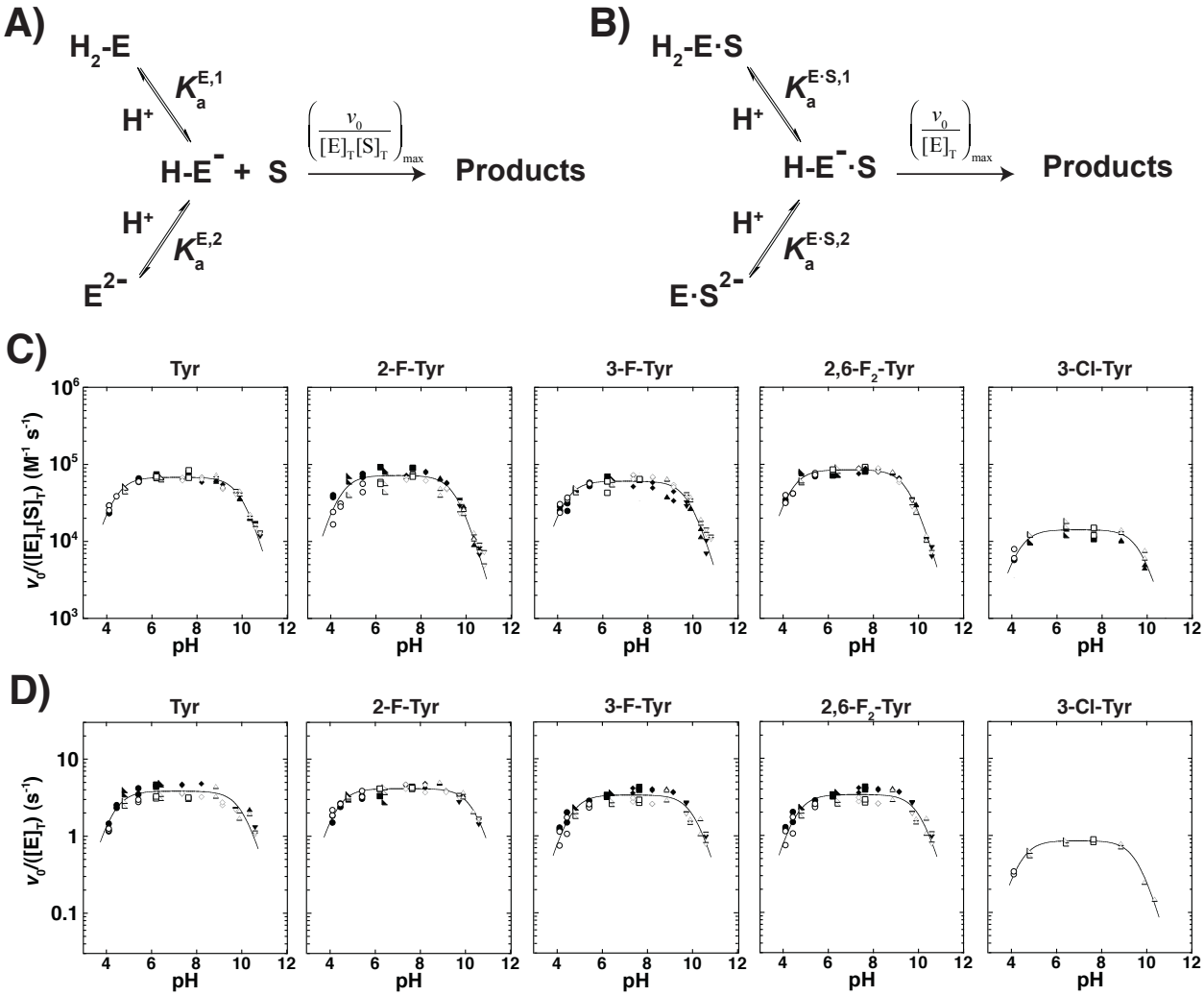

Figure S3. pH dependencies of activity of semisynthetic KSI variants with 5(10)-EST. A,B) Reaction schemes depicting an inactivating protonation ($pK_a^{E,1}$ or $pK_a^{E\cdot S,1}$) and an inactivating deprotonation ($pK_a^{E,2}$ or $pK_a^{E\cdot S,2}$) under subsaturating (A) or saturating (B) conditions. C,D) pH-dependent activity measurements with 5(10)-EST under subsaturating (C) and saturating conditions (D). Data were collected as described in Materials and Methods and fit to the reaction schemes in (A) and (B). Open and closed symbols represent substrate concentrations of 4.7 μM and 9.4 μM used to measure subsaturating activity and 300 μM and 600 μM used to measure saturating activity, respectively. The following buffers were used: sodium acetate (circles), sodium succinate (right triangles), sodium phosphate (squares), sodium tricine (diamonds),

sodium glycine (upward-facing triangles), sodium carbonate (downward-facing triangles). The inactivating protonation and deprotonation pK_a values from each fit are given in Tables 1 and 2 respectively.

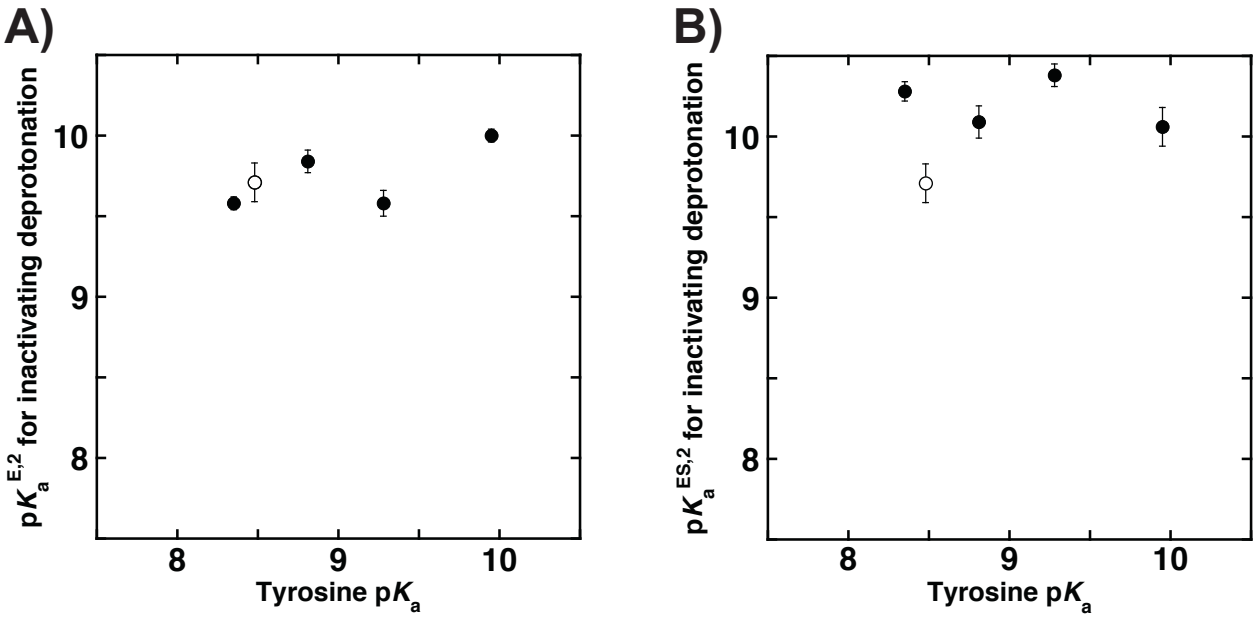

Figure S4. The inactivating deprotonation pK_a values observed in pH dependencies of activity with 5(10)-EST show no dependence on tyrosine side chain pK_a. Subsaturating and saturating pK_a values are shown in (A) and (B) respectively.

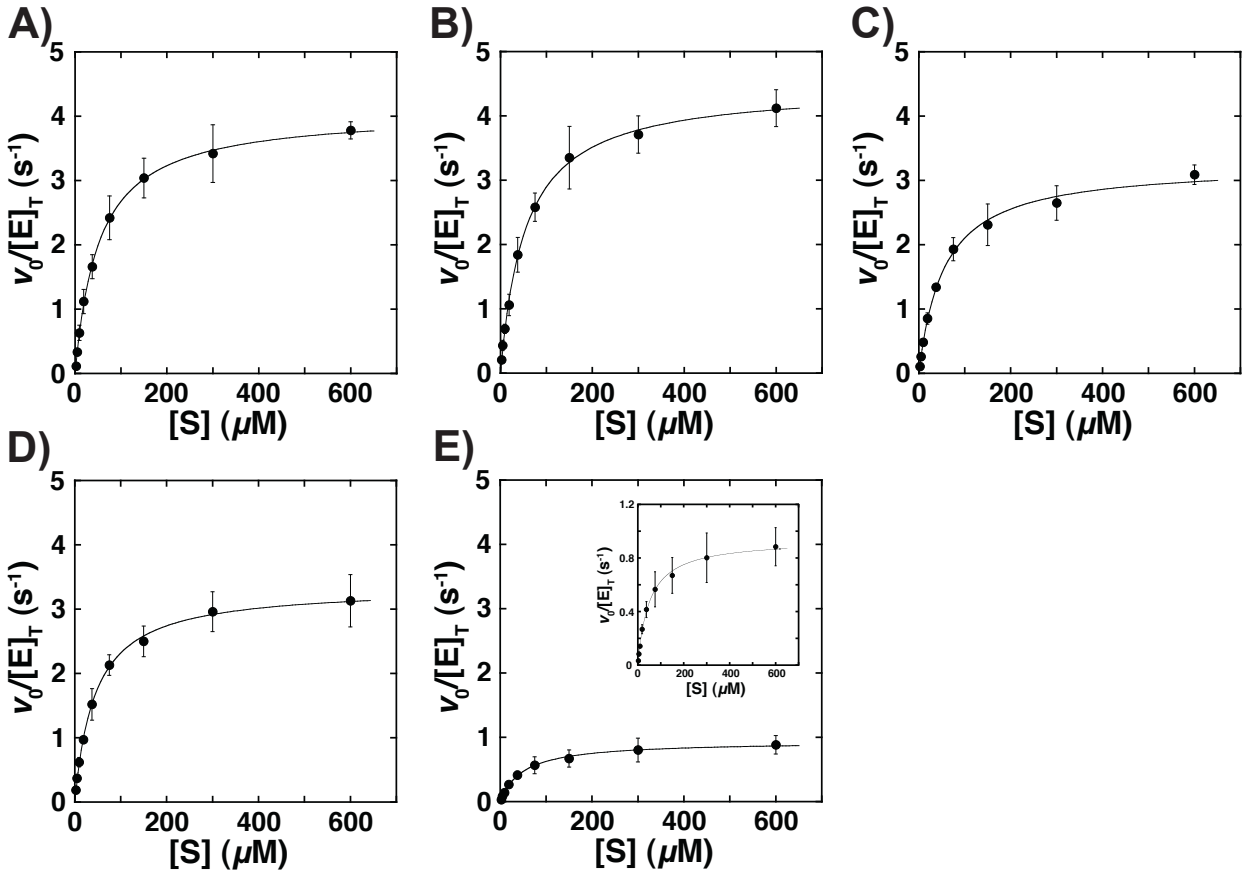

Figure S5. Initial rates of product formation with 2 – 600 μM 5(10)-EST and semisynthetic KSI containing (A) Tyr, (B) 2-F-Tyr, (C) 3-F-Tyr, (D) 2,6-F_2-Tyr, (E) 3-Cl-Tyr at position 16. The inset in (E) shows the same values plotted on an expanded ordinate for clarity. Error bars represent standard deviations from 3-4 independent experiments using enzyme concentrations varied over a 6- to 10-fold range. Data were collected as described in Materials and Methods and fit to the Michaelis-Menten equation. Averaged Michaelis-Menten parameters corresponding to the data presented are given in Table S3.

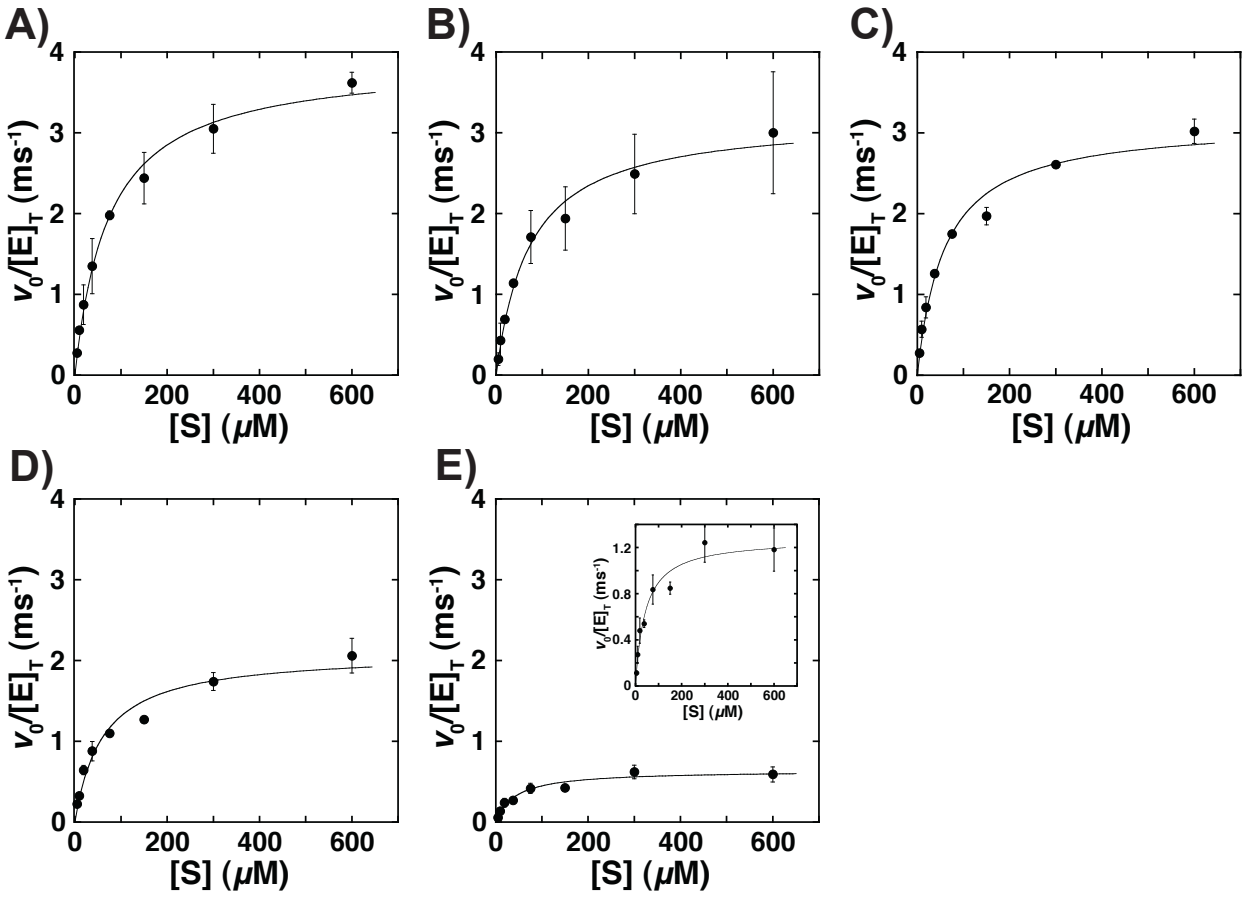

Figure S6. Initial rates of product formation with 5 – 600 μM 5-AND and semisynthetic KSI containing (A) Tyr, (B) 2-F-Tyr, (C) 3-F-Tyr, (D) 2,6-F_2-Tyr, (E) 3-Cl-Tyr at position 16. The inset in (E) shows the same values plotted on an expanded axis for clarity. Error bars represent standard deviations from 2-3 independent experiments using enzyme concentrations over a 6- to 10-fold range. Data were collected as described in Materials and Methods and fit to the Michaelis-Menten equation. Averaged Michaelis-Menten parameters corresponding to the data presented are given in Table S4.

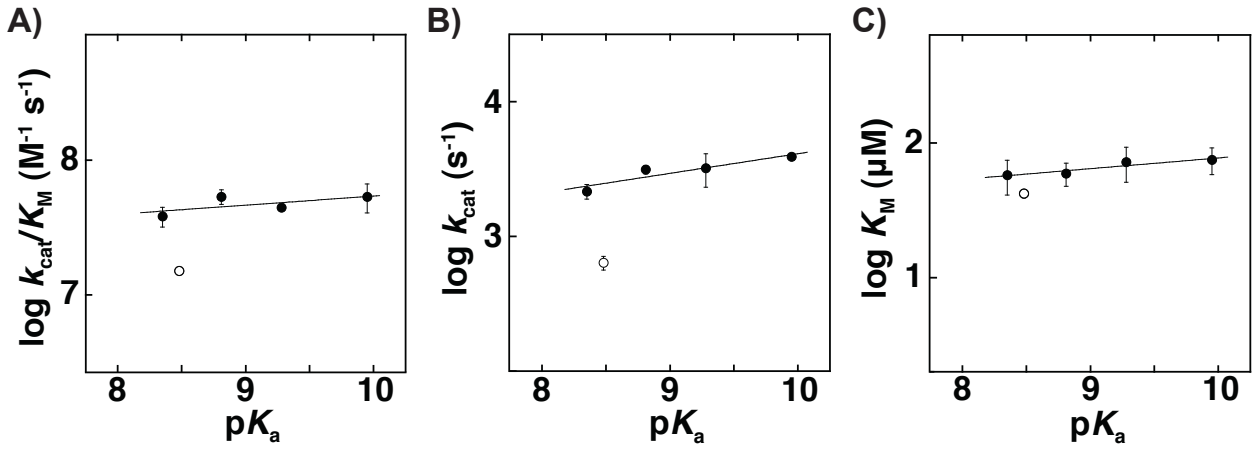

Figure S7. Dependence of (A) k_{cat}/K_M, (B) k_{cat} and (C) K_M for isomerization of 5-AND on the side chain pK_a of substituted tyrosine. Tyr and F-Tyr containing variants are shown as closed circles, and 3-Cl-Tyr is shown as open circles. Error bars correspond to standard deviations from 3-4 independent experiments using different enzyme concentrations. Lines of best fit were determined for Tyr and F-Tyr data, not including 3-Cl-Tyr. The slopes in (A)-(C) are 0.07 ± 0.05, 0.15 ± 0.06, and 0.08 ± 0.03, respectively.

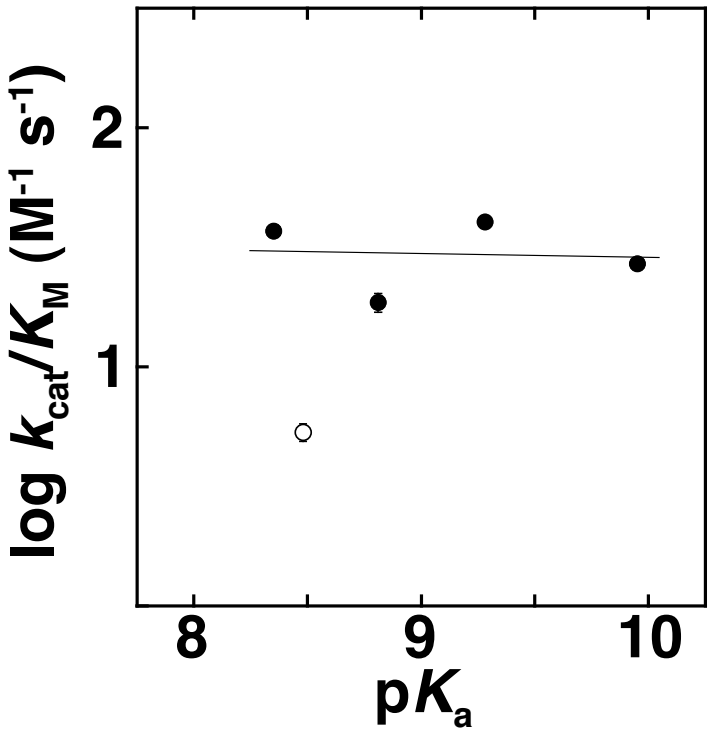

Figure S8. Dependence of k_{cat}/K_M for isomerization of 3-cyclohexen-1-one on the side chain pK_a of substituted tyrosine. Tyr and F-Tyr containing variants are shown as closed circles, and 3-Cl-Tyr is shown as open circles. Error bars correspond to standard deviations from 2-3 independent experiments using different enzyme concentrations. The slope of the line, drawn only through Tyr and F-Tyr data points, is -0.02 ± 0.15.

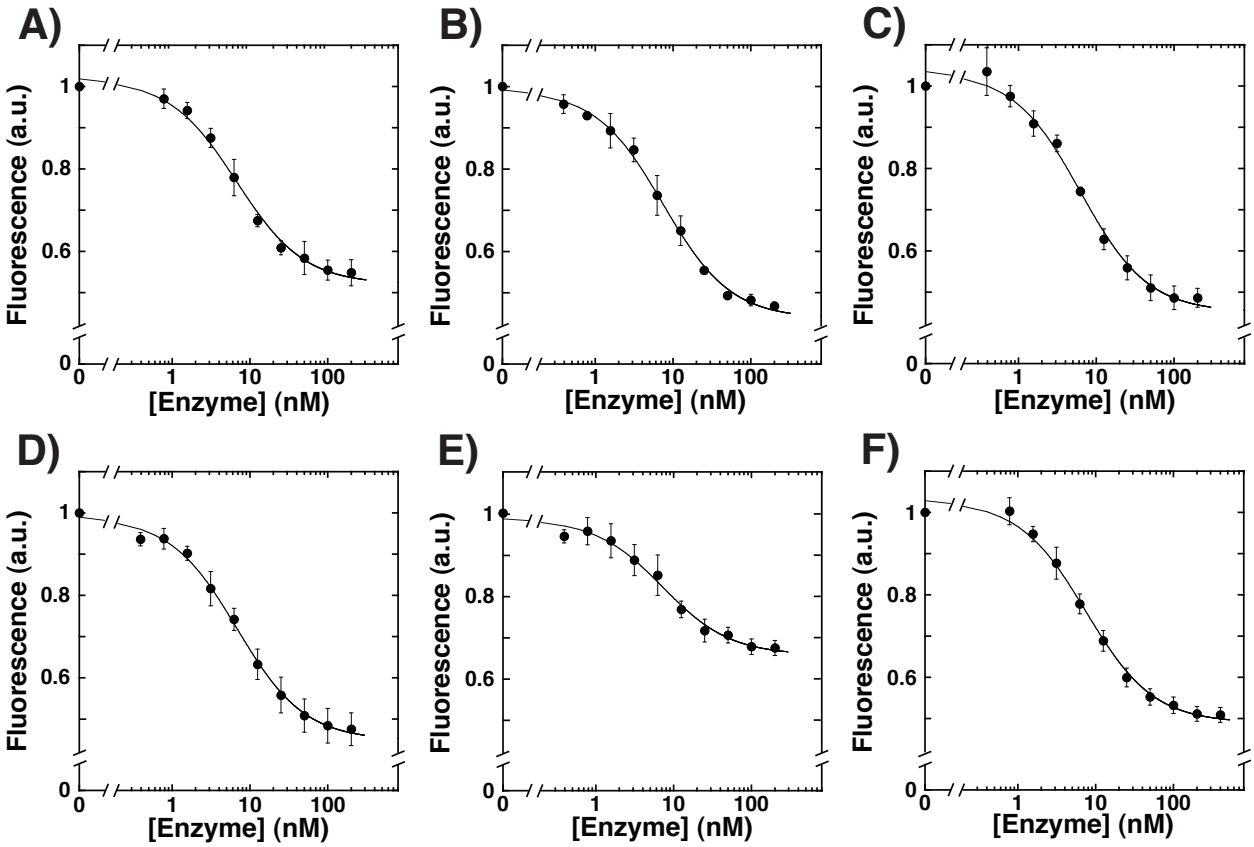

Figure S9. Determination of equilenin affinity for KSI variants containing a D40N mutation by monitoring quenching of fluorescence of EqA488-1 (0.1 nM) upon adding 0 – 200 nM enzyme. Data corresponding to expressed KSI are shown in (A), while data corresponding to semisynthetic KSI containing Tyr, 2-F-Tyr, 3-F-Tyr, 2,6-F_2-Tyr and 3-Cl-Tyr are shown in (B) through (F) respectively. Observed fluorescence values in each experiment were normalized to the fluorescence with no enzyme present. Error bars represent standard deviations from 4-12 replicates. Data were collected and fit to a quadratic binding isotherm as described in Materials and Methods. Affinities determined from fits to the data presented are given in Table S6. Conditions: 10 mM potassium phosphate, 0.1 mM sodium·EDTA, μ = 100 mM (KCl), pH 7.2

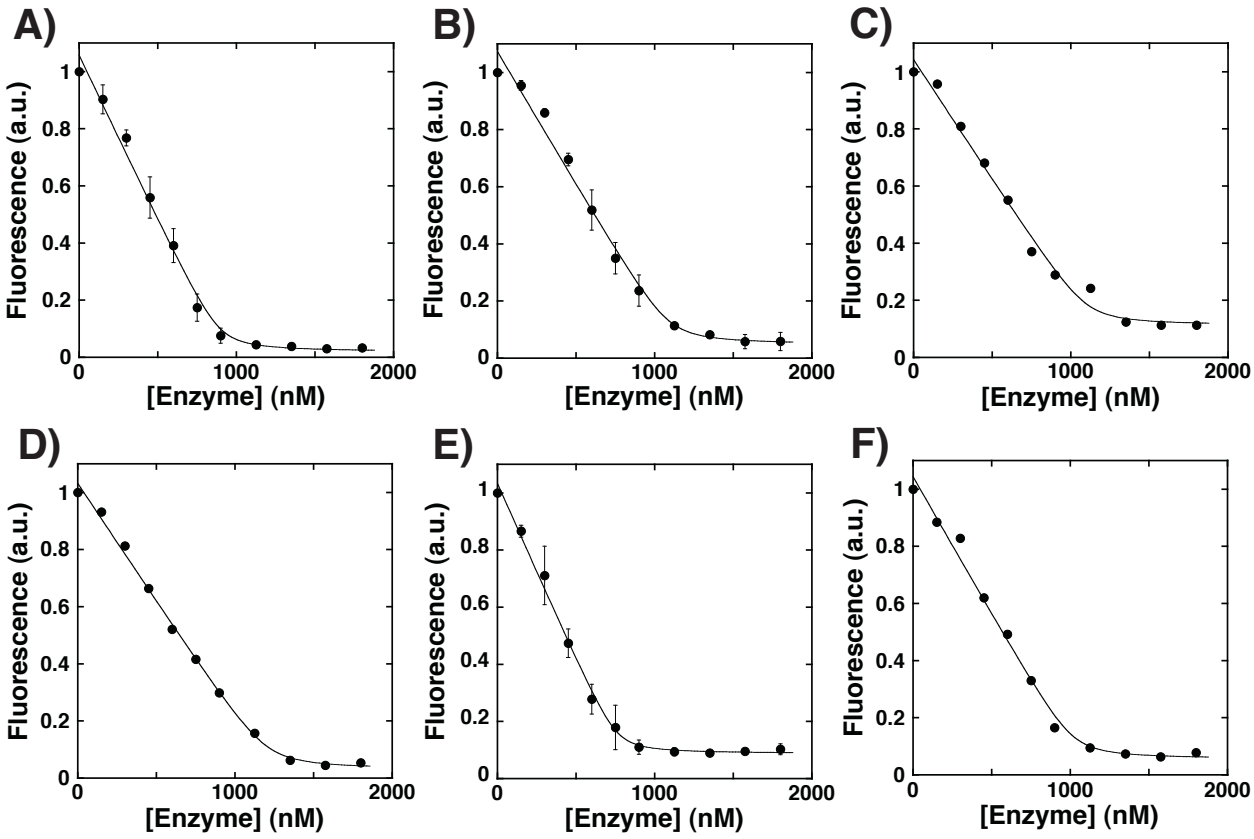

Figure S10. Titrations to determine the fraction of active enzyme by monitoring fluorescence of 900 nM equilenin with 0 – 1800 nM KSI containing a D40N mutation and other mutations inserted to facilitate semisynthesis as described in the main text. Data corresponding to expressed KSI are shown in (A), while data corresponding to semisynthetic KSI containing Tyr, 2-F-Tyr, 3-F-Tyr, 2,6-F_2-Tyr and 3-Cl-Tyr are shown in (B) through (F) respectively. Observed fluorescence values in each experiment were normalized to the fluorescence with no enzyme present. Error bars represent standard deviations from 2-3 independent replicates. Data were collected and fit to a quadratic binding isotherm as described in Materials and Methods. Values of the fraction of enzyme that can bind equilenin determined from fits to the data presented are given in Table S7. Conditions: 10 mM potassium phosphate, 0.1 mM sodium·EDTA, μ = 100 mM (KCl), 5% DMSO (v/v) pH 7.2.

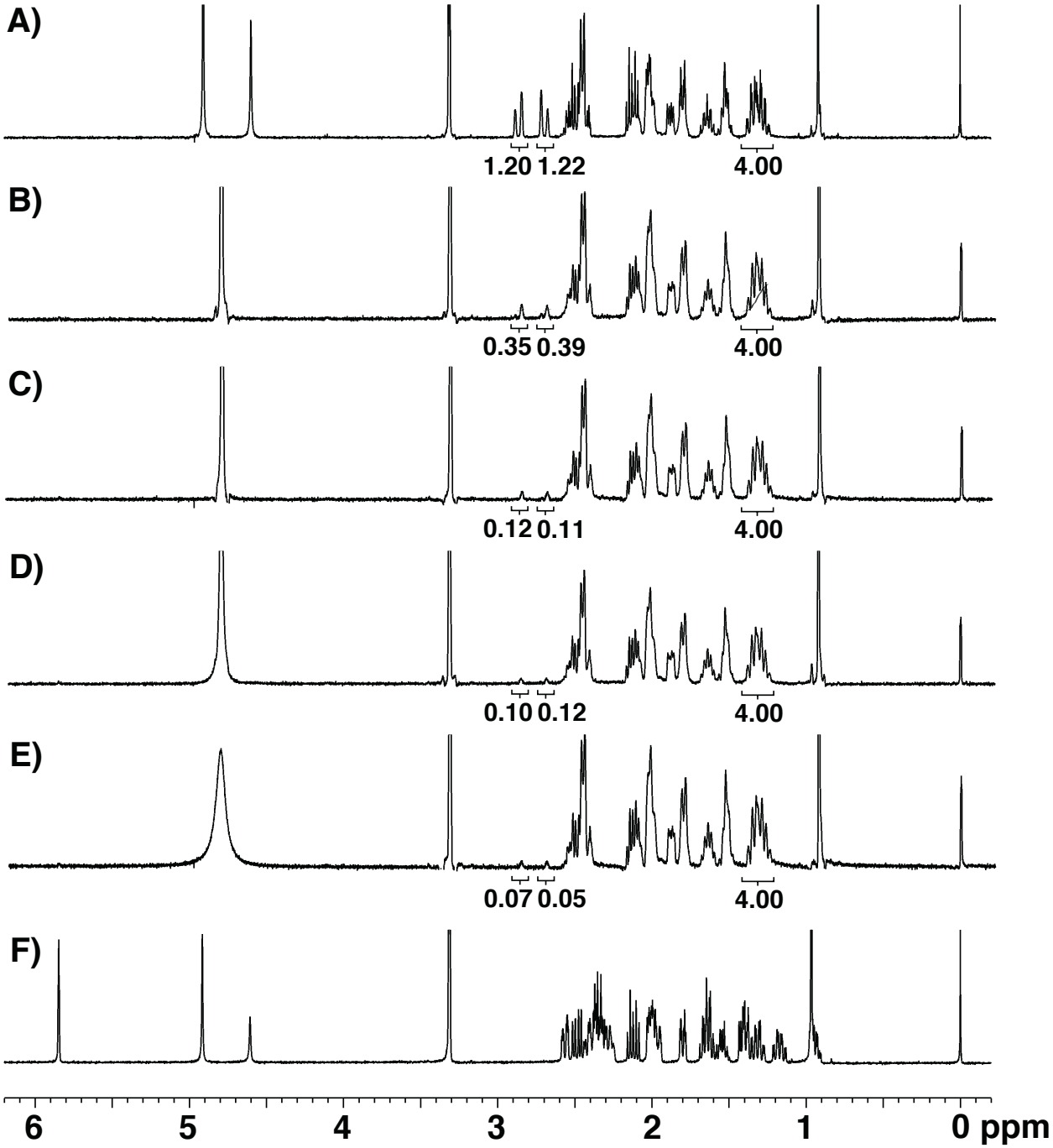

Figure S11. Incubation of protiated (^{1}H) 5(10)-EST with 1 mM NaOD in D_2O leads to H/D exchange of α-protons without formation of conjugated product (4-EST) over 18 minutes. (A)-(E) ^{1}H NMR (500 MHz) spectra for 35 mM 5(10)-EST with (A) no added base, (B)-(E) 1 mM NaOD after 2, 4, 9 and 18 minutes respectively. (F) ^{1}H NMR (500 MHz) spectrum for 35 mM 4-EST with no added base. All spectra were recorded in 9:1 CD_3OD:D_2O (v/v).

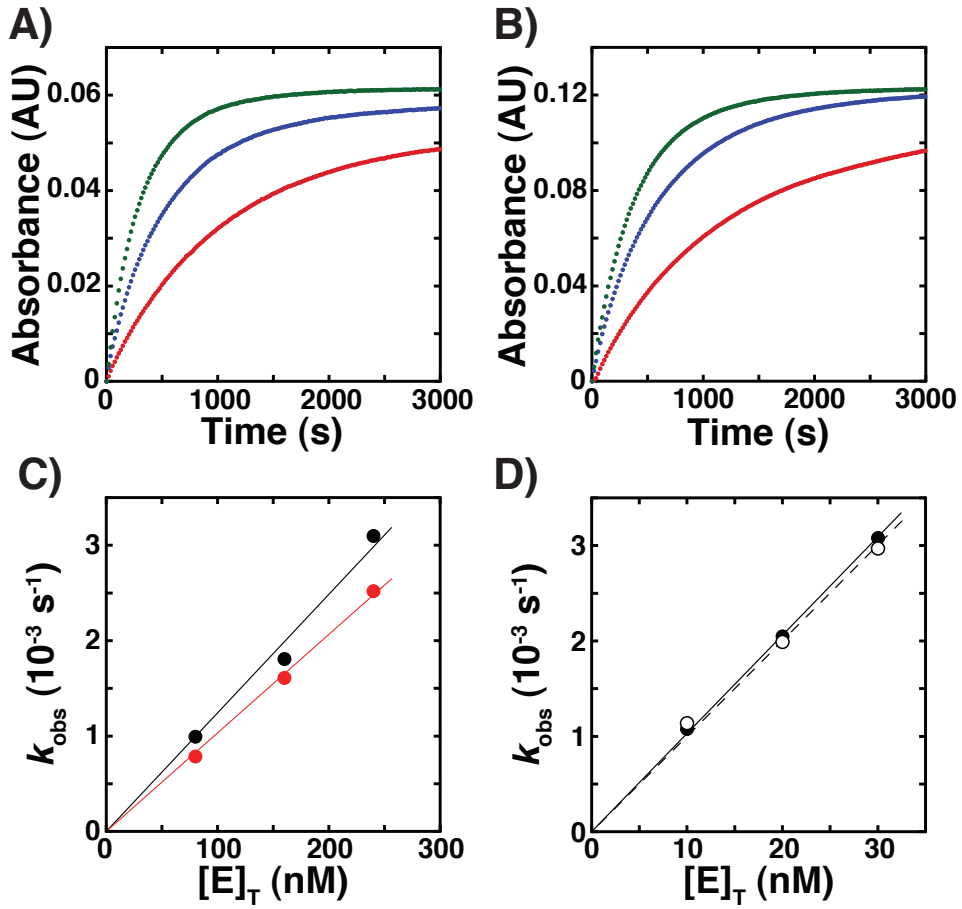

Figure S12. A,B) Product formation observed upon diluting 4,4-dideuterated 5(10)-EST, generated by incubating 5(10)-EST with 1 mM NaOD in D_2O, to subsaturating final concentrations into deuterated buffer with WT semisynthetic KSI. Substrate at 6 μM (A) or 12 μM (B) with 80 nM (red), 160 nM (blue) and 240 nM (green) enzyme. (C) Rate constants obtained from fits of the data in (A) and (B) to single exponentials. The values of k_{cat}/K_M from the fits shown are 1.23×10^4 M^{-1} s^{-1} (6 μM substrate, black circles) and 1.04×10^4 M^{-1} s^{-1} (12 μM substrate, blue circles). (D) Activity of WT semisynthetic KSI with subsaturating 5(10)-EST (6 μM) that had been incubated first with either H_2O (open) or 1 mM NaOH in H_2O (closed). The values of k_{cat}/K_M from the fits shown are 1.00×10^5 M^{-1} s^{-1} (open) and 1.03×10^5 M^{-1} s^{-1} (closed). Conditions: 40 mM potassium phosphate, 1 mM sodium·EDTA, 2% DMSO (v/v), pH 7.2 (H_2O) or pD 7.6 (D_2O).

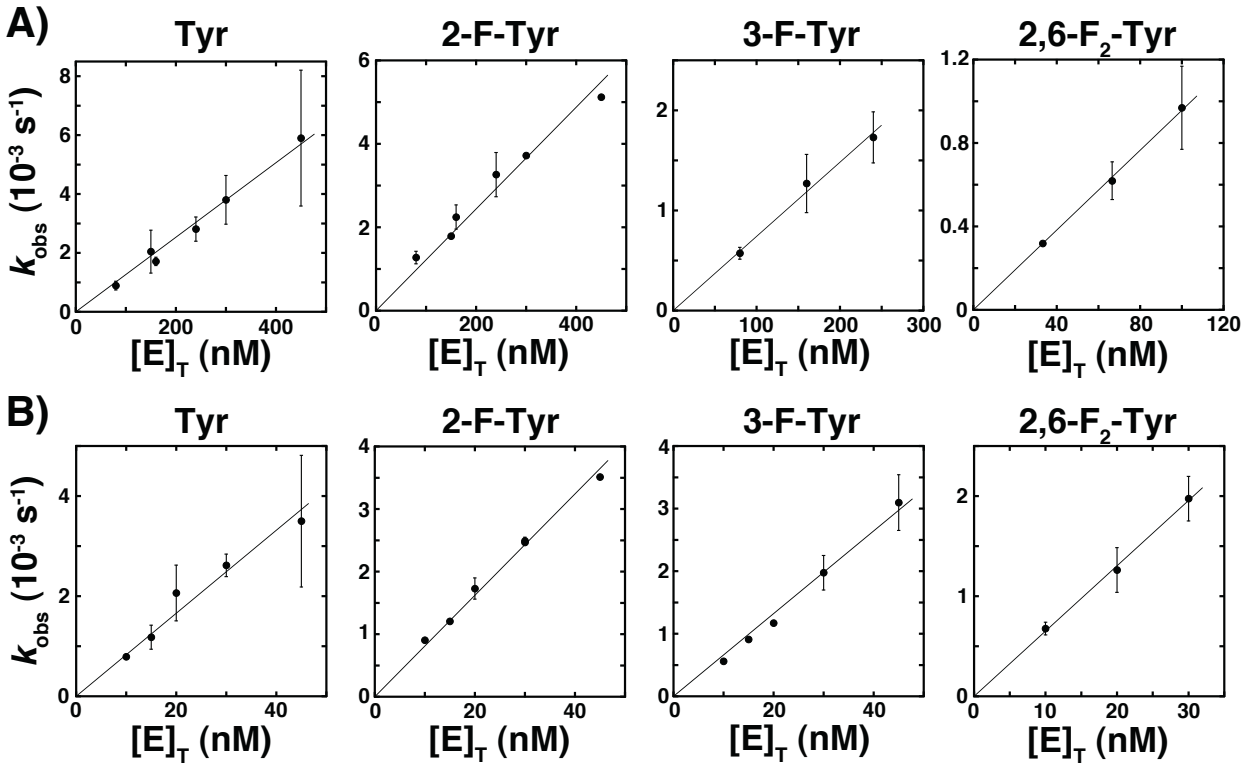

Figure S13. Activity of semisynthetic KSIs with subsaturating 4,4-dideuterated 5(10)-EST in D_2O and protiated 5(10)-EST in H_2O. (A) Rate constants for product formation for 4,4-dideuterated 5(10)-EST in deuterated buffer with semisynthetic KSI variants. (B) Rate constants for product formation for protiated 5(10)-EST in protiated buffer with semisynthetic KSI variants. Substrate concentrations used were 6 or 12 μM. Error bars correspond to standard deviations from 2-4 independent experiments. Averaged values of k_{cat}/K_M from the best fits shown are presented in Table 4. Conditions: 40 mM potassium phosphate, 1 mM sodium·EDTA, 2% DMSO (v/v), pH 7.2 (H_2O) or pD 7.6 (D_2O).

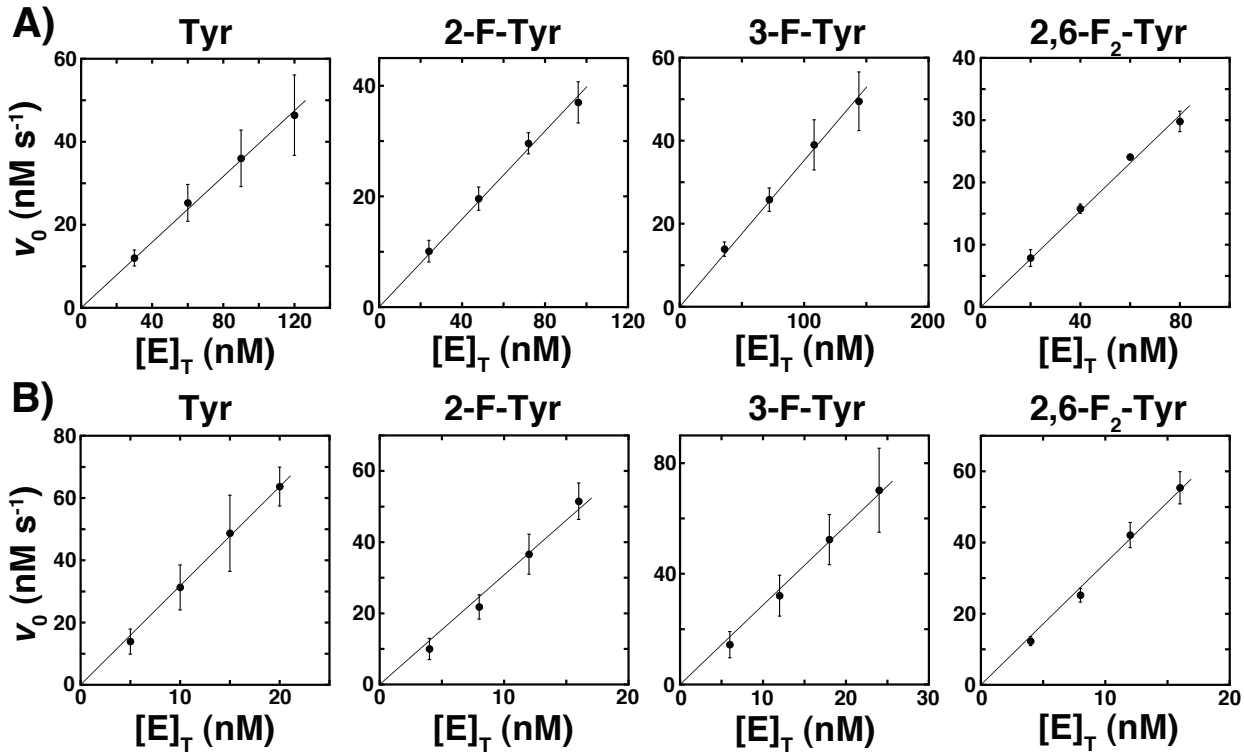

Figure S14. Activity of semisynthetic KSIs with saturating (300 μM) 4,4-dideuterated 5(10)-EST in D_2O and protiated 5(10)-EST in H_2O. (A) Rate constants for product formation observed for 4,4-dideuterated 5(10)-EST in deuterated buffer with semisynthetic KSI variants. (B) Rate constants for product formation observed for protiated 5(10)-EST in protiated buffer with semisynthetic KSI variants. Error bars correspond to standard deviations from 2-4 independent experiments. Averaged values of v_0/[E] from the best fits shown are presented in Table 5. Conditions: 40 mM potassium phosphate, 1 mM sodium·EDTA, 2% DMSO (v/v), pH 7.2 (H_2O) or pD 7.6 (D_2O).

Table S1. Substrate Concentrations used in Kinetic Characterizations of KSI Variants

Experiment	Substrate	Concentrations used (μM)	K_M range (μM)[a]
pH-dependent activity measurements	5(10)-EST	4.7, 9.4, 300, 600	36 to 56
Michaelis-Menten kinetics	5(10)-EST	2.3, 4.7, 9.4, 18.8, 37.5, 75, 300, 600	36 to 56
	5-AND	4.7, 9.4, 18.8, 37.5, 75, 300, 600	42 to 75
k_{cat}/K_M determination for 3-cyclohexen-1-one	3-cyclohexen-1-one	1, 5 mM	100 to 500 mM
Solvent isotope effect measurements	5(10)-EST	2.3, 4.7, 9.4, 18.8, 37.5, 300	36 to 56
Primary kinetic isotope effect measurements	5(10)-EST	6, 12, 300	36 to 56

[a] K_M values for 5(10)-EST and 5-AND for the KSI variants characterized in this manuscript are reported in Tables S2 to S4. K_M values for 3-cyclohexen-1-one were determined by Schwans *et al.*[7] for wild type and several oxyanion hole mutants of KSI from *Pseudomonas putida*.

Table S2. Michaelis-Menten Parameters for KSI-catalyzed Isomerization of 5(10)-EST by expressed proteins[a]

Enzyme	k_{cat}/K_M (M^{-1} s^{-1})	k_{cat} (s^{-1})	K_M (μM)
Wild type[b]	$(3.3 \pm 0.7) \times 10^5$	10 ± 1	30 ± 4
Y32F	$(1.7 \pm 0.2) \times 10^5$	6 ± 1	36 ± 2
R15K/D21N/D24C/Y32F/ C69S/C81S/C97S (WT)	$(1.3 \pm 0.3) \times 10^5$	6 ± 1	45 ± 5

[a] Conditions: 40 mM potassium phosphate, 1 mM EDTA, 2% DMSO (v/v), pH 7.2. Standard deviations are from at least three experiments using different enzyme concentrations.

[b] Values from Schwans *et al.*[6]

Table S3. Michaelis-Menten Parameters for Isomerization of 5(10)-EST by Semisynthetic KSIs[a]

Residue at position 16	k_{cat}/K_M (M^{-1} s^{-1})	k_{cat} (s^{-1})	K_M (μM)
Tyr (WT)	$(7.8 \pm 0.7) \times 10^4$	4.1 ± 0.3	52 ± 1
2-F-Tyr	$(7.9 \pm 1.1) \times 10^4$	4.4 ± 0.6	56 ± 6
3-F-Tyr	$(6.0 \pm 0.4) \times 10^4$	3.3 ± 0.3	55 ± 5
2,6-F_2-Tyr	$(7.5 \pm 0.6) \times 10^4$	3.4 ± 0.4	44 ± 2
3-Cl-Tyr	$(1.9 \pm 0.3) \times 10^4$	0.9 ± 0.2	50 ± 6

[a]Conditions: 40 mM potassium phosphate, 1 mM EDTA, 2% DMSO (v/v), pH 7.2. Standard deviations are from 3-4 independent experiments using different enzyme concentrations, each using nine different substrate concentrations varied in two-fold increments from 2.3 to 600 μM. Enzyme concentrations ranged from 5 to 60 nM for tyrosine and fluorotyrosine containing KSI variants, and from 30 to 180 nM for 3-chlorotyrosine containing KSI.

Table S4. Michaelis-Menten Parameters for Isomerization of 5-AND by Semisynthetic KSIs[a]

Residue at position 16	k_{cat}/K_M (M^{-1} s^{-1})	k_{cat} (s^{-1})	K_M (μM)
Tyr (WT)	$(5.4 \pm 1.3) \times 10^7$	$(3.9 \pm 0.1) \times 10^3$	75 ± 17
2-F-Tyr	$(4.5 \pm 0.1) \times 10^7$	$(3.2 \pm 0.9) \times 10^3$	72 ± 20
3-F-Tyr	$(5.4 \pm 0.7) \times 10^7$	$(3.1 \pm 0.2) \times 10^3$	59 ± 12
2,6-F_2-Tyr	$(3.8 \pm 0.6) \times 10^7$	$(2.2 \pm 0.3) \times 10^3$	58 ± 17
3-Cl-Tyr	$(1.5 \pm 0.1) \times 10^7$	$(6.4 \pm 0.7) \times 10^2$	42 ± 3

[a]Conditions: 40 mM potassium phosphate, 1 mM EDTA, 2% DMSO (v/v), pH 7.2. Standard deviations are from 2-3 independent experiments using different enzyme concentrations, each using eight different substrate concentrations varied in two-fold increments from 4.7 to 600 μM. Enzyme concentrations ranged from 30 to 180 pM for tyrosine and fluorotyrosine containing KSI variants, and from 180 pM to 1 nM for 3-chlorotyrosine containing KSI.

Table S5. Values of k_{cat}/K_M for Isomerization of 3-cyclohexen-1-one by Semisynthetic KSIs[a]

Residue at position 16	k_{cat}/K_M (M^{-1} s^{-1})
Tyr (WT)	2.7 ± 0.1
2-F-Tyr	4.0 ± 0.1
3-F-Tyr	1.9 ± 0.2
2,6-F_2-Tyr	3.7 ± 0.1
3-Cl-Tyr	(5.3 ± 0.4) × 10^{-1}

[a]Conditions: 4 mM potassium phosphate, 0.1 mM EDTA, 2% DMSO (v/v), pH 7.2. Standard deviations are from 2-3 independent experiments using different enzyme concentrations varied over a 4-fold range up to 300 nM, each using 1.0 and 5.0 mM substrate.

Table S6. Affinities of Expressed and Semisynthetic KSI variants for EqA488-1, a Fluorescent Analog of Equilenin[a]

Residue at position 16	K_d (nM)
Tyr (expressed)	6.8 ± 1.1
Tyr (semisynthetic)	7.5 ± 2.3
2-F-Tyr	6.2 ± 0.5
3-F-Tyr	6.6 ± 0.8
2,6-F_2-Tyr	7.1 ± 1.9
3-Cl-Tyr	7.5 ± 0.8

[a] Conditions: 0.1 nM EqA488-1, 10 mM potassium phosphate, 0.1 mM sodium·EDTA, μ = 100 mM (KCl), pH 7.2. Enzymes contain the D40N mutation, as well as the mutations R15K/D21N/D24C/Y32F/C69S/C81S/C97S as described in the main text. Standard deviations are from 4-12 independent replicates.

Table S7. Fraction of Expressed and Semisynthetic KSI variants that Binds Equilenin[a]

Residue at position 16	Fraction of enzyme that binds equilenin
Tyr (expressed)	1.01 ± 0.04
Tyr (semisynthetic)	0.83 ± 0.09
2-F-Tyr	0.82 ± 0.04
3-F-Tyr	0.75 ± 0.02
2,6-F_2-Tyr	1.18 ± 0.04
3-Cl-Tyr	0.88 ± 0.04

[a] Conditions: 900 nM equilenin, 10 mM potassium phosphate, 0.1 mM sodium·EDTA, μ = 100 mM (KCl), 5% DMSO (v/v), pH 7.2. All enzymes listed contain the D40N mutation, as well as the mutations R15K/D21N/D24C/Y32F/C69S/C81S/C97S as described in the main text. Standard deviations are from 2-3 independent replicates.

NMR spectra and Masses of Protected Tyrosines

1. (*S*)-2-((*tert*-butoxycarbonyl)amino)-3-(2-fluoro-4-hydroxyphenyl)propanoic acid (*N*-Boc-2-fluorotyrosine). ^{1}H NMR ($CDCl_3$); δ 6.94 (dt, J = 25.7 Hz, 8.5 Hz, 1 H), 6.50 (m, 2 H), 5.97 (d, J = 8.2 Hz, 0.4 H), 5.79 (br s, 1 H), 5.21 (d, J = 8.2 Hz, 0.6 H), 4.53 (q, J = 7.1 Hz, 0.6 H), 4.43 (q, J = 7.1 Hz, 0.4 H), 3.00 (m, 2 H), 1.41 (s, 9 H). ^{13}C NMR ($CDCl_3$); δ 175.79, 175.50, 162.98, 161.01, 156.78, 155.99, 132.19, 114.31, 111.74, 103.44 (d, J = 23.1 Hz), 82.48, 81.04, 54.96, 54.16, 31.56, 31.15, 28.46, 28.30. ^{19}F NMR ($CDCl_3$); δ -115.69 (t, J = 8.7 Hz, 0.63 F), -115.82 (t, J = 8.7 Hz, 0.36 F). Calculated mass (M-H) = 298.12; found 298.19 (ESI-MS).

^{1}H NMR, 500 MHz ($CDCl_3$)

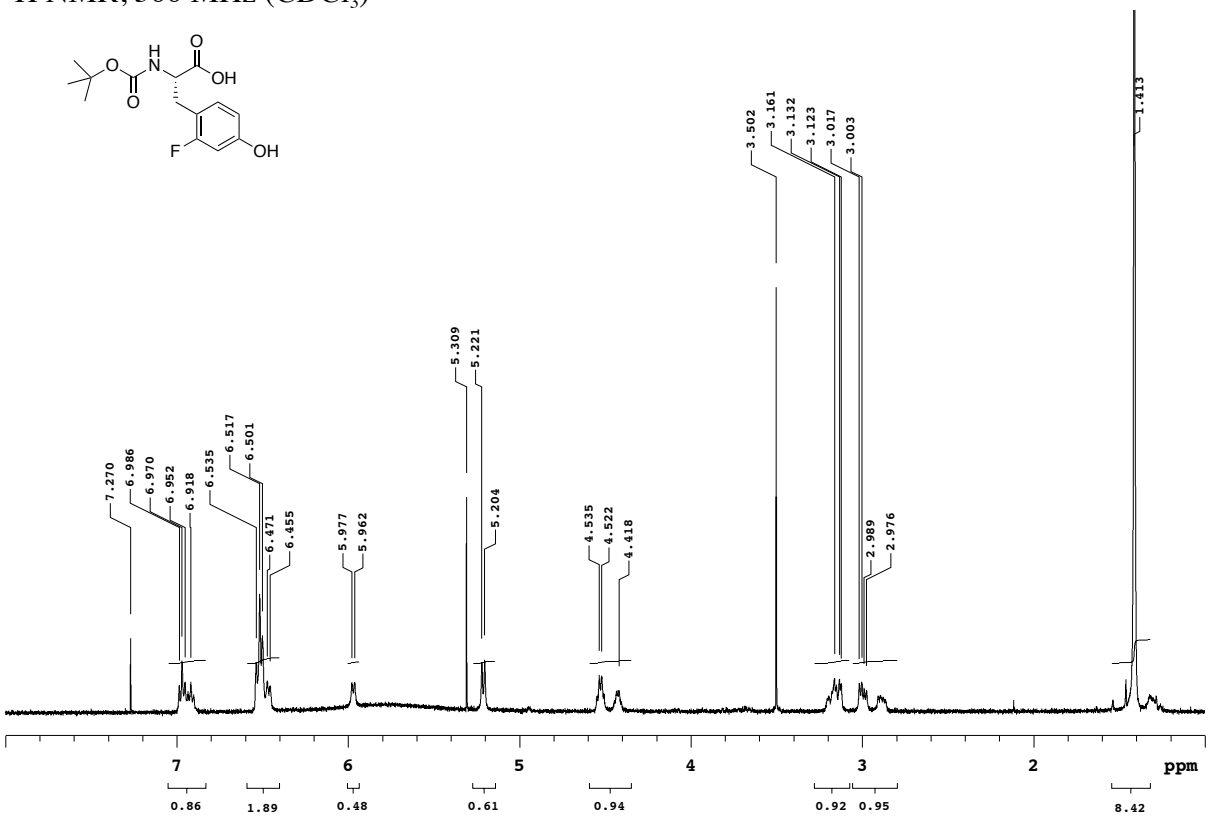

^{13}C NMR, 125.7 MHz ($CDCl_3$)

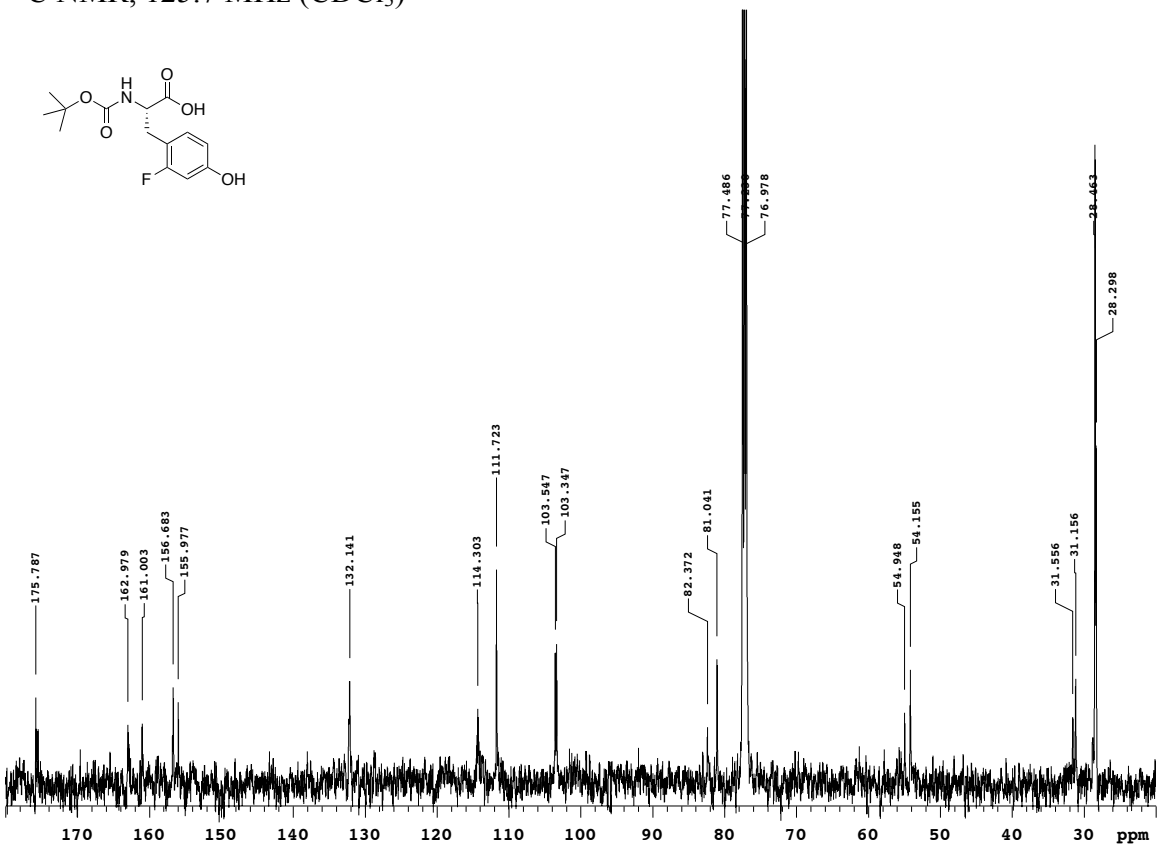

^{19}F NMR, 470.5 MHz ($CDCl_3$)

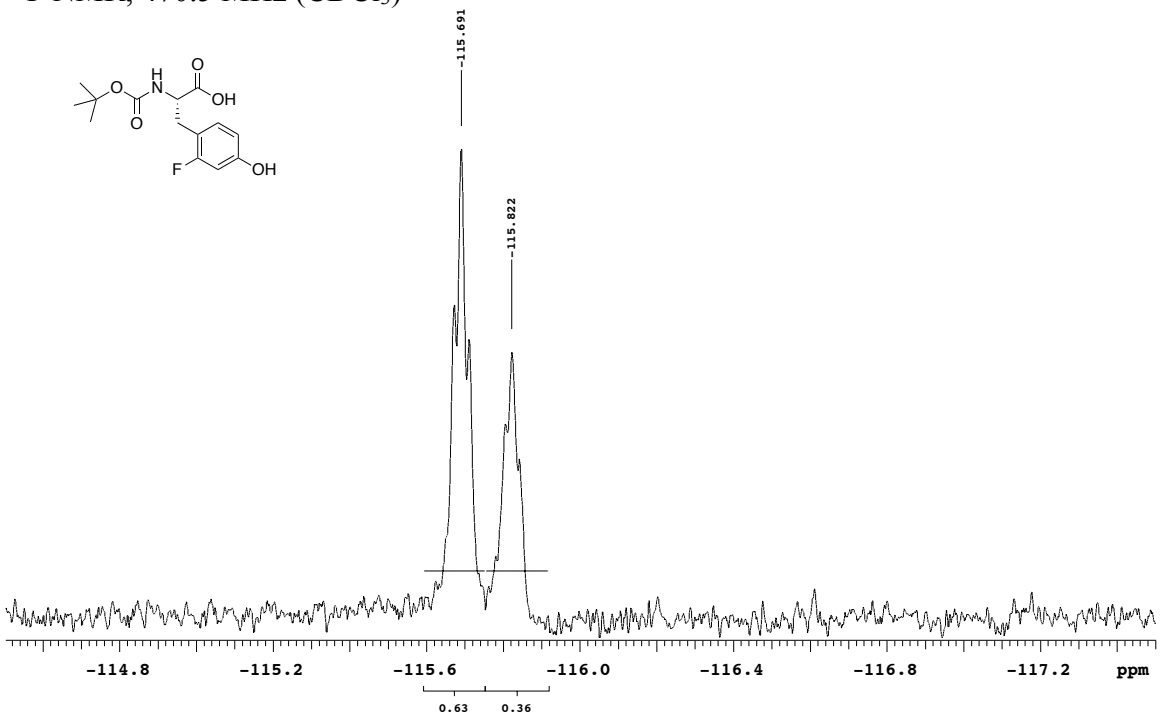

2. (*S*)-2-((*tert*-butoxycarbonyl)amino)-3-(3-fluoro-4-hydroxyphenyl)propanoic acid (*N*-Boc-3-fluorotyrosine). ^{1}H NMR ($CDCl_3$); 6.82 (m, 4 H), 6.17 (d, *J* = 8 Hz, 0.38 H), 5.16 (d, *J* = 8 Hz, 0.64 H), 4.55 (m, 0.64 H), 4.35 (m, 0.36 H), 2.97 (m, 2 H), 1.42 (s, 6.1 H), 1.38 (s, 2.9 H). ^{13}C NMR ($CDCl_3$); 175.86, 175.69, 156.86, 155.90, 152.14, 150.23, 143.0 (d, *J* = 13.7 Hz), 128.54 (m), 125.77 (m), 117.79, 116.87 (d, *J* = 18.5 Hz), 82.4 ppm, 81.04, 56.04, 54.51, 37.65, 37.21, 28.44, 28.27. ^{19}F NMR ($CDCl_3$); -138.72 (t, *J* = 10.1 Hz, 0.38 F), -138.96 (t, *J* = 10.1 Hz, 0.60 F). Calculated mass (M-H) = 298.12; found 298.37 (ESI-MS).

^{1}H NMR, 500 MHz ($CDCl_3$)

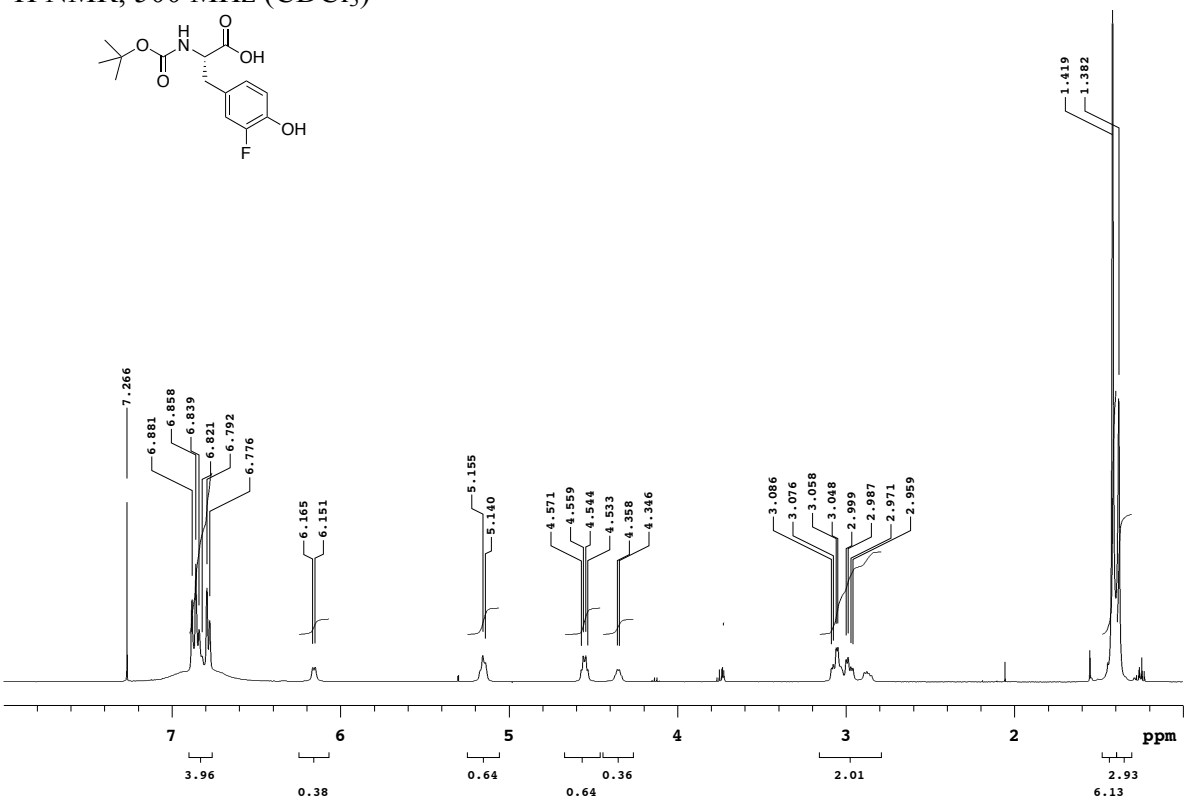

^{13}C NMR, 125.7 MHz ($CDCl_3$)

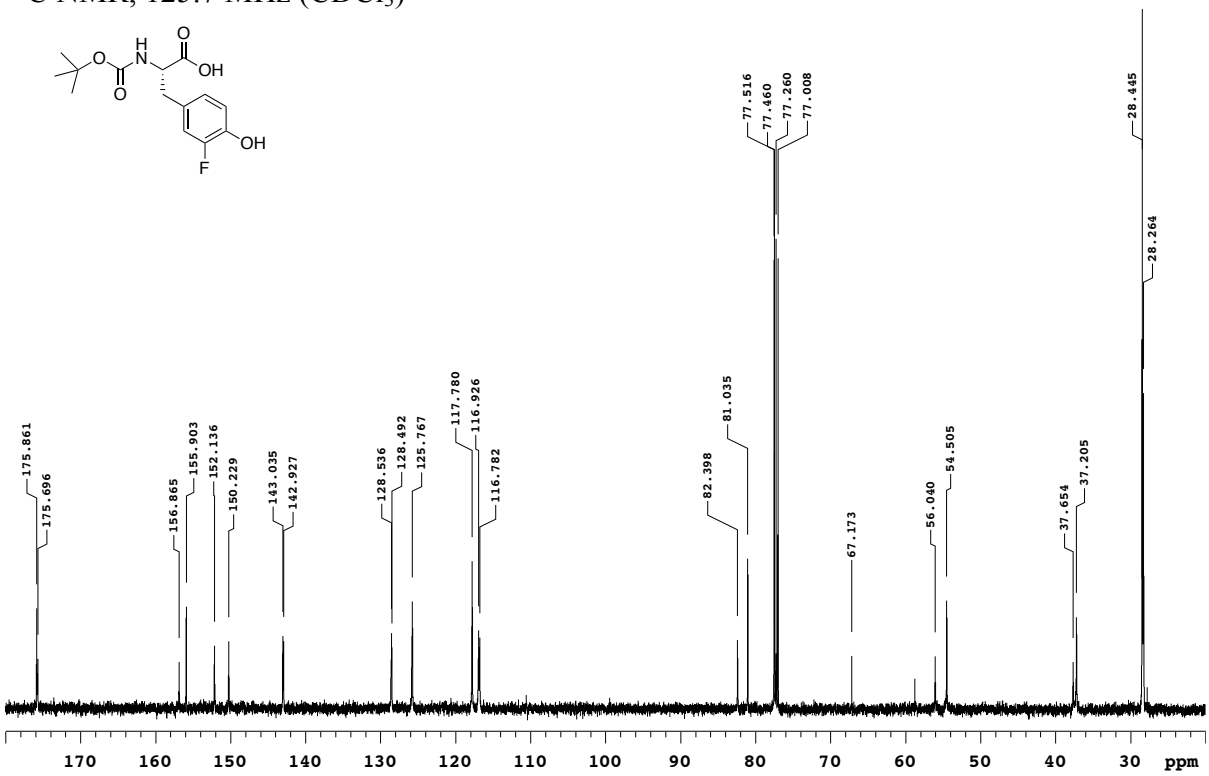

^{19}F NMR, 470.5 MHz ($CDCl_3$)

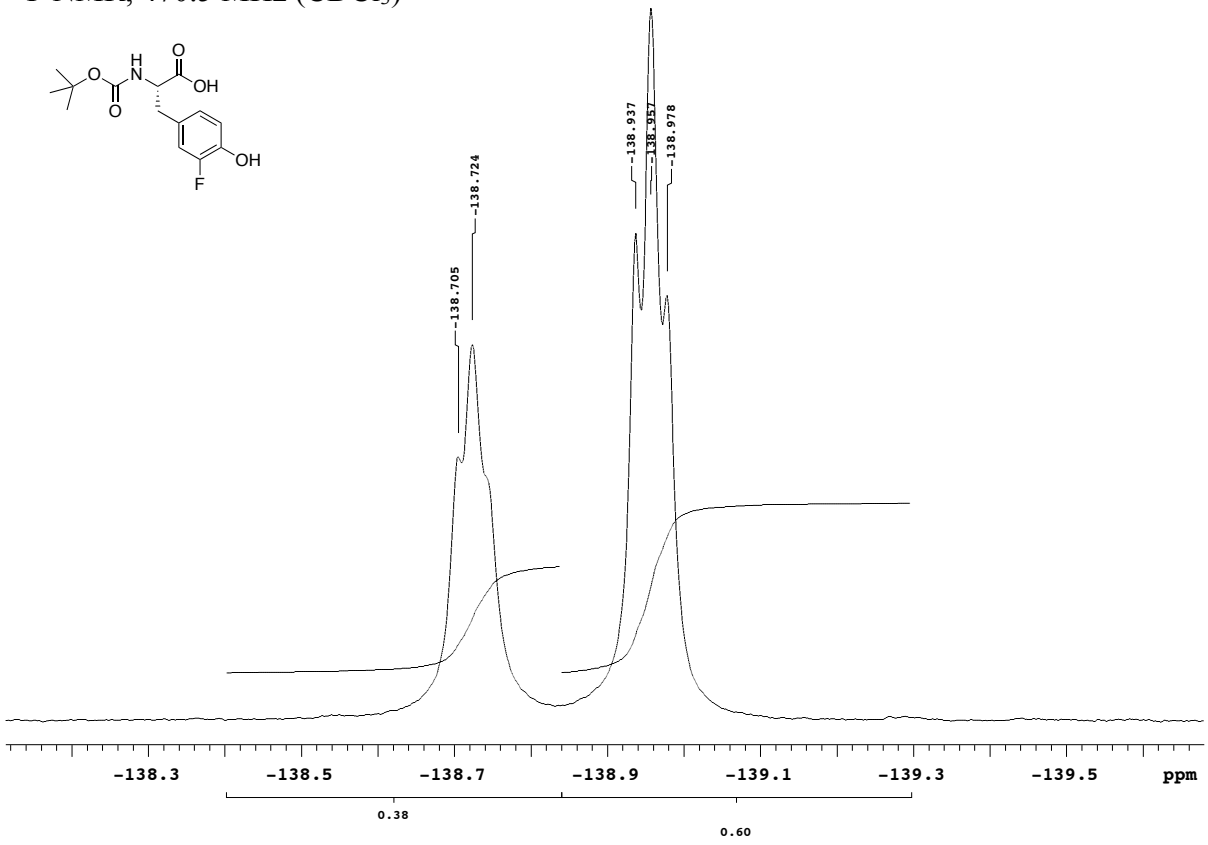

3. (*S*)-2-((*tert*-butoxycarbonyl)amino)-3-(2,6-difluoro-4-hydroxyphenyl)propanoic acid (*N*-Boc-2,6-difluorotyrosine). ^{1}H NMR (Acetone-d_6); 6.44 (d, J = 9.3 Hz, 2 H), 6.03 (d, J = 8.4 Hz, 0.76 H), 5.75 (d, J = 8.4 Hz, 0.19 H), 4.40 (m, 0.79 H), 4.31 (m, 0.21 H), 3.15 (dd, J = 14.5 Hz, 5.1 Hz, 1 H), 2.98 (dd, J = 13.9 Hz, 8.2 Hz, 1 H), 1.35 (s, 9 H). ^{13}C NMR (Acetone-d_6); 173.1, 164.2 (d, J = 12.7 Hz), 162.2 (d, J = 12.7 Hz), 158.8 (t, J = 15.3 Hz), 156.1, 104.6 (t, J = 22 Hz), 99.7 (dd, J = 22 Hz, 7.1 Hz), 79.3, 79.2, 55.1, 54.0, 28.45, 28.21, 25.97, 25.46. ^{19}F NMR (Acetone-d_6); -114.81 (d, J = 9.3 Hz, 1.6 F), -114.92 (d, J = 9.3 Hz, 0.4 F). Calculated mass (M-H) = 316.12; found 316.36 (ESI-MS).

^{1}H NMR, 500 MHz (Acetone-d_6)

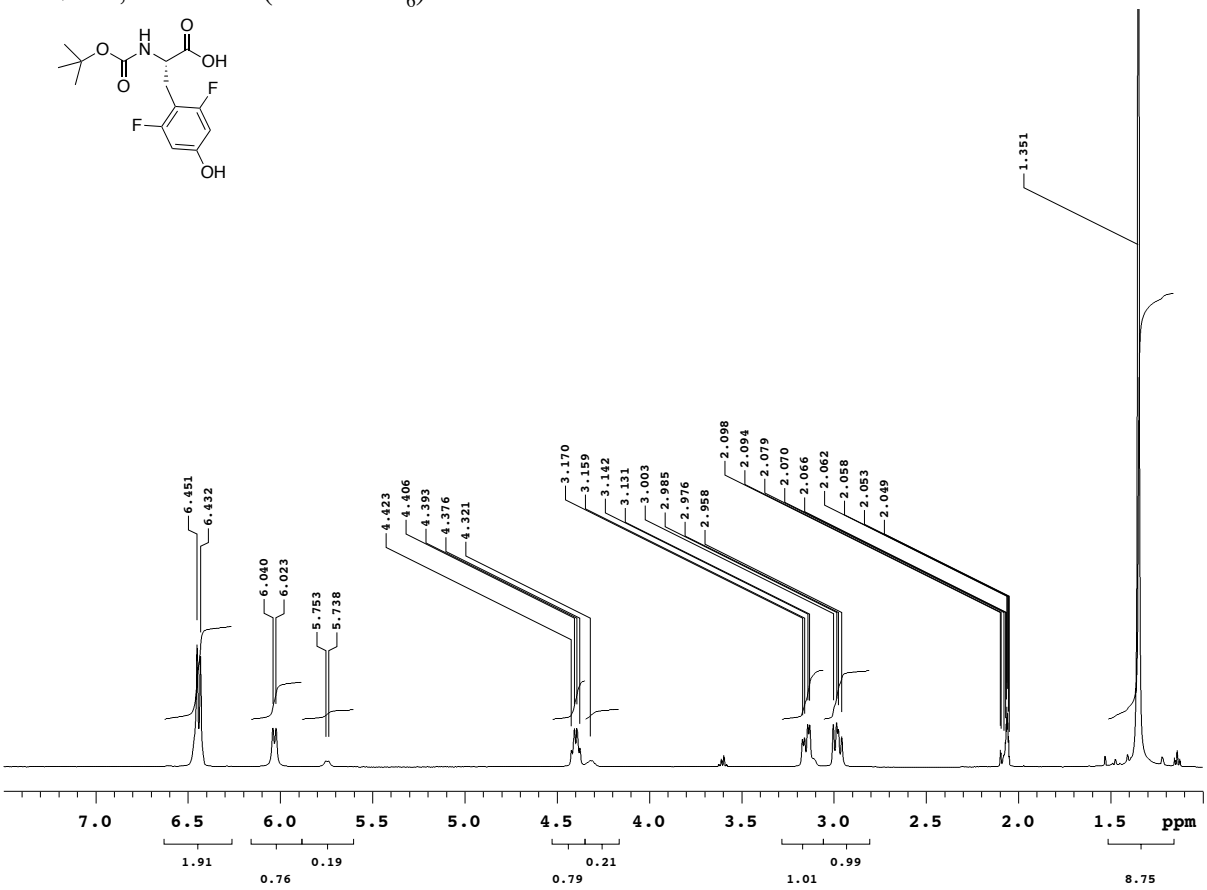

^{13}C NMR, 125.7 MHz (Acetone-d_6)

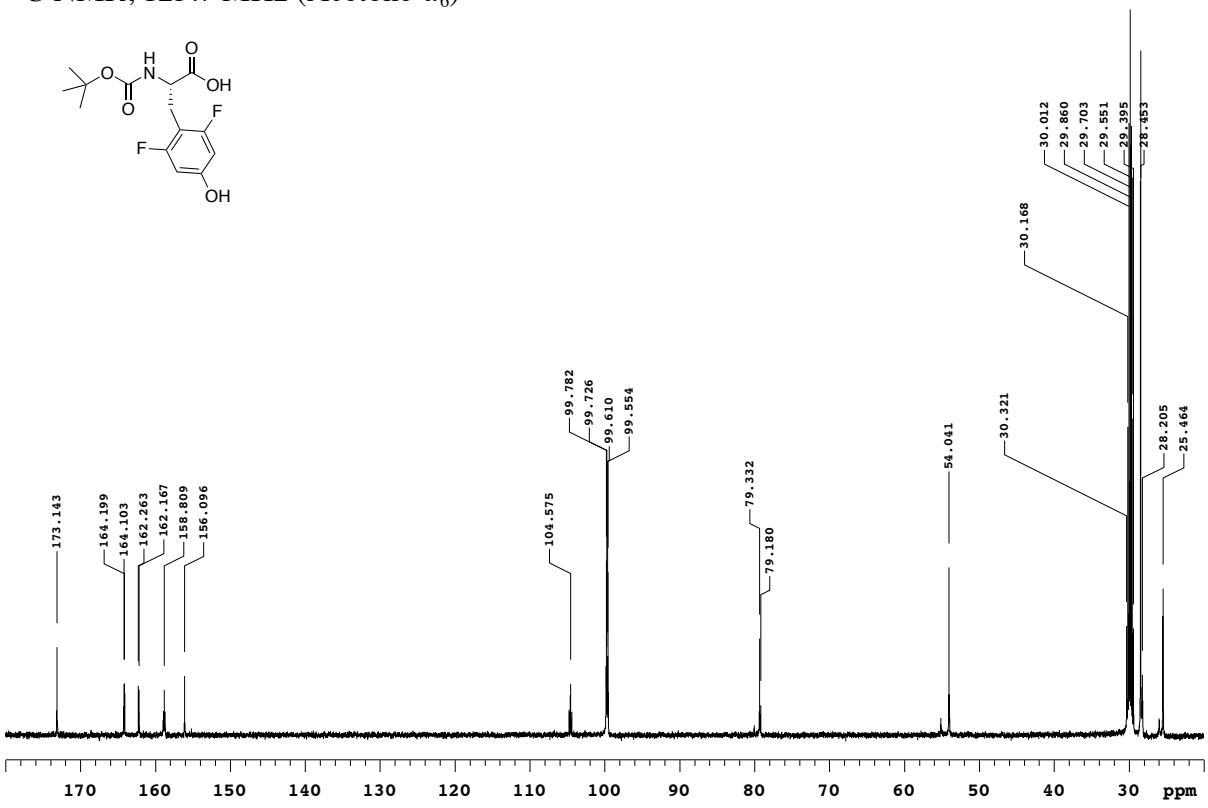

^{19}F NMR, 470.5 MHz (Acetone-d_6)

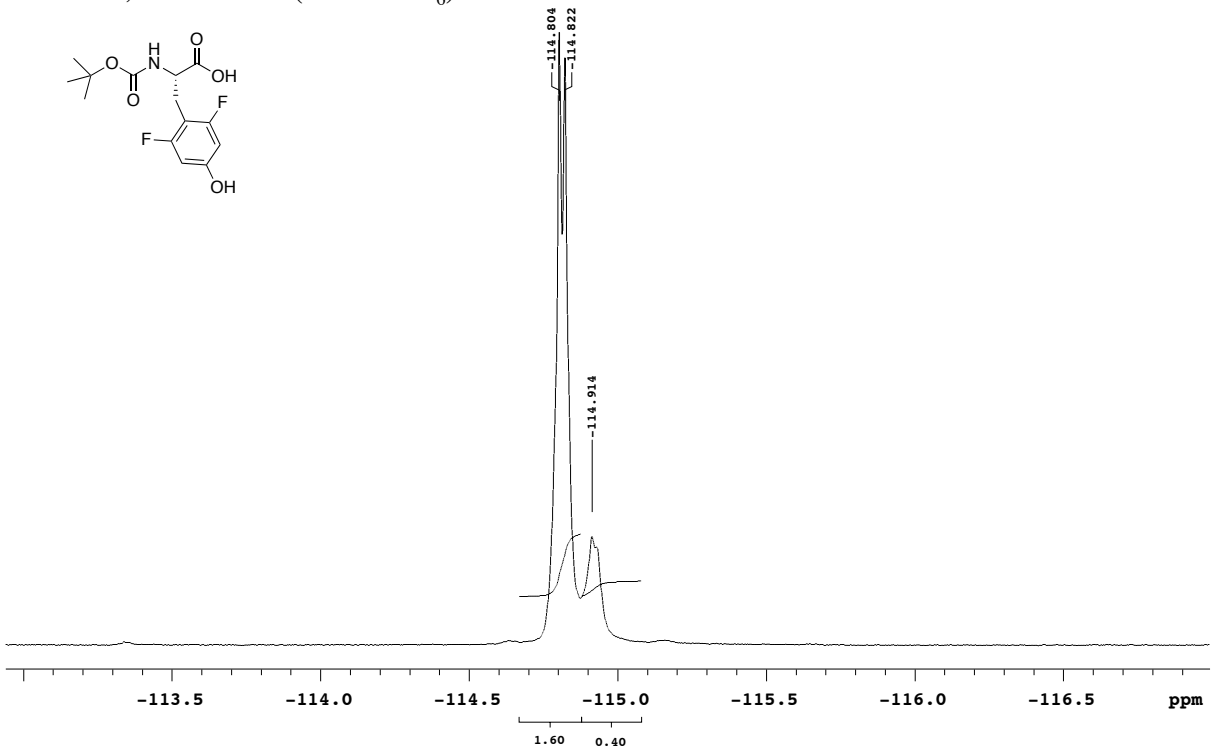

4. (*S*)-2-((*tert*-butoxycarbonyl)amino)-3-(3-chloro-4-hydroxyphenyl)propanoic acid (*N*-Boc-3-chlorotyrosine). ^{1}H NMR ($CDCl_3$); δ 7.14 (d, J = 17.3 Hz, 1 H), 6.97 (dd, J = 8.45 Hz, 1.41 Hz, 1 H), 6.91 (d, J = 8.45 Hz, 1 H), 6.29 (d, J = 7.63 Hz, 0.35 H), 5.05 (d, J = 7.63 Hz, 0.62 H), 4.55 (q, J = 6.11 Hz, 0.62 H), 4.33 (q, J = 6.11 Hz, 0.29 H), 2.97 (m, 2H), 1.42 (s, 5.6 H), 1.34 (s, 2.8 H). ^{13}C NMR ($CDCl_3$); δ 177.41, 176.26, 176.04, 155.60, 150.78, 130.1, 129.25, 129.54, 120.12, 116.61, 82.11, 80.73, 56.12, 54.50, 37.97, 37.04, 28.51, 28.27. Calculated mass (E-H) = 314.09; found 314.20 (ESI-MS).

^{1}H NMR, 500 MHz ($CDCl_3$)

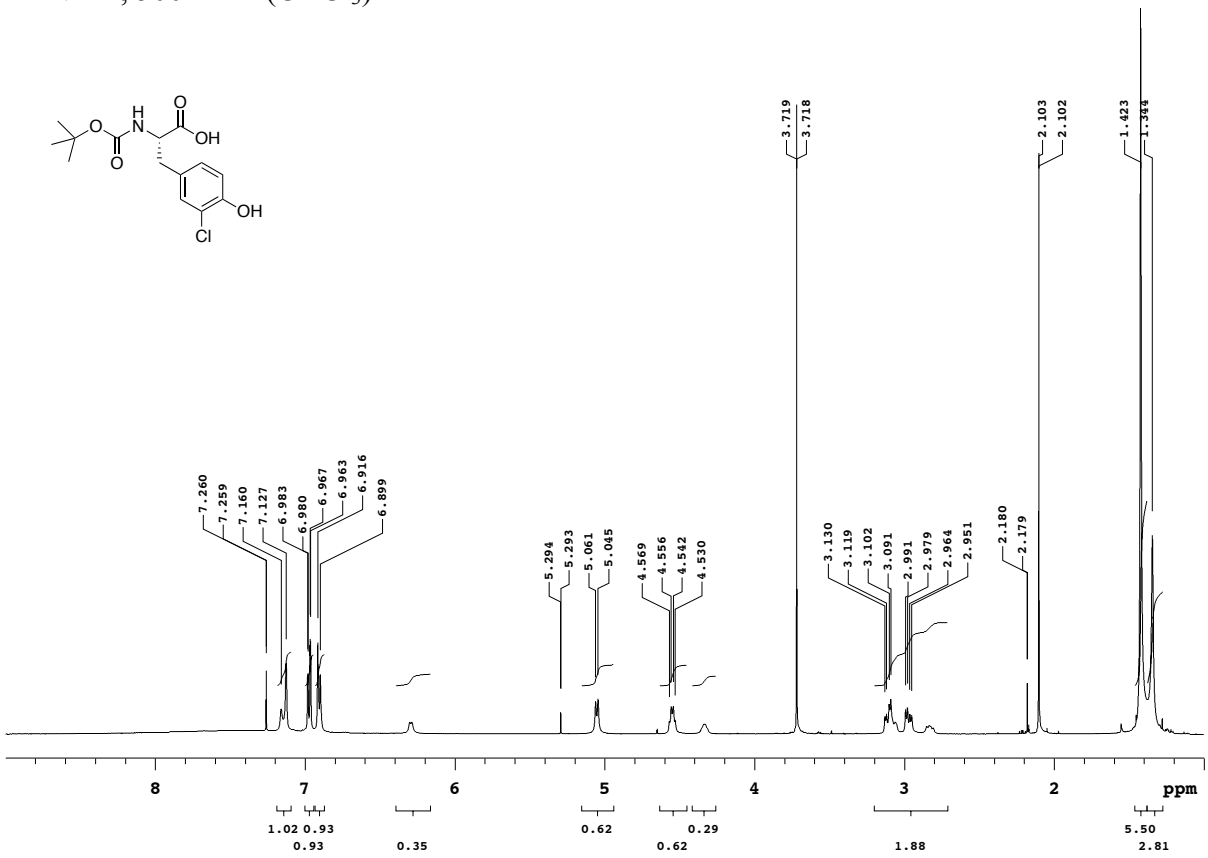

^{13}C NMR, 125.7 MHz ($CDCl_3$)

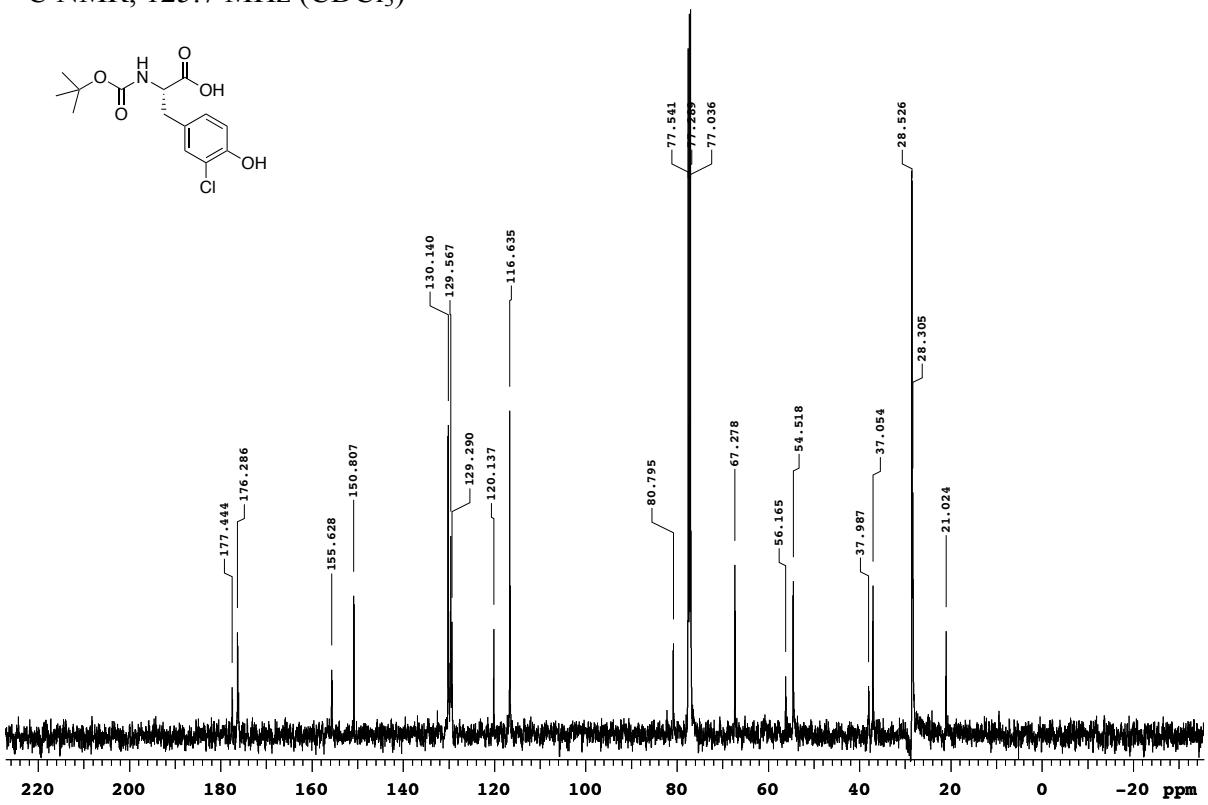

5. (*S*)-2-((*tert*-butoxycarbonyl)amino)-3-(4-((*tert*-butyldimethylsilyl)oxy)-2-fluorophenyl)propanoic acid. ^{1}H NMR ($CDCl_3$); δ 7.73 (br s, 1 H), 7.03 (t, J = 8.5 Hz, 1 H), 6.56 (m, 2 H), 5.02 (d, J = 8.2 Hz, 0.48 H), 4.54 (q, J = 7.6 Hz, 0.53 H), 4.45 (q, J = 7.6 Hz, 0.34 H), 3.0 (m, 2 H), 1.40 (s, 5.7 H), 1.29 (s, 3.6 H), 0.96 (s, 9 H), 0.19 (s, 6 H). ^{13}C NMR ($CDCl_3$); δ 176.60, 175.87, 163.22, 160.75, 156.64, 155.63, 156.31 (d, J = 11.4 Hz), 132.24, 131.89, 116.2, 115.95, 107.78 (d, J = 21.0 Hz), 81.62, 80.48, 55.00, 54.01, 53.67, 33.01, 31.15, 28.48, 28.20, 25.82, 18.38, -4.25. ^{19}F NMR ($CDCl_3$); δ -115.84 (t, J = 9.8 Hz, 0.6 H), -116.16 (t, J = 9.8 Hz, 0.4 H). Calculated mass (M-H) = 412.20; found 412.19 (ESI-MS).

^{1}H NMR, 400 MHz ($CDCl_3$)

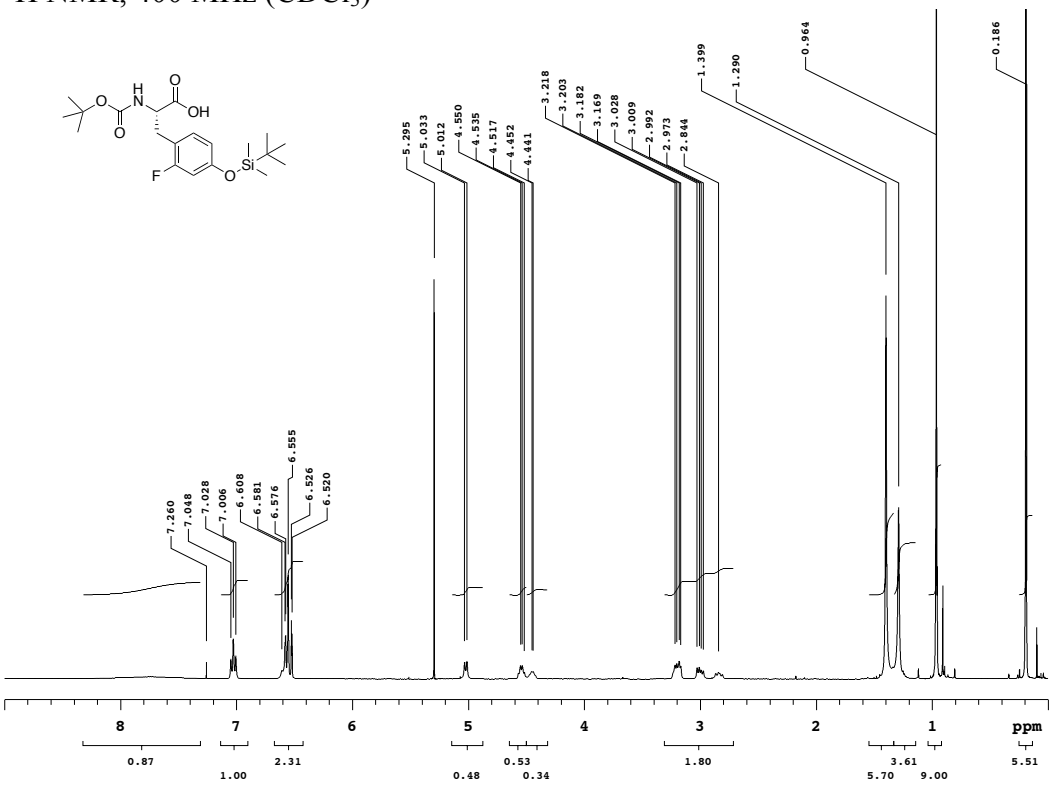

^{13}C NMR, 100.6 MHz ($CDCl_3$)

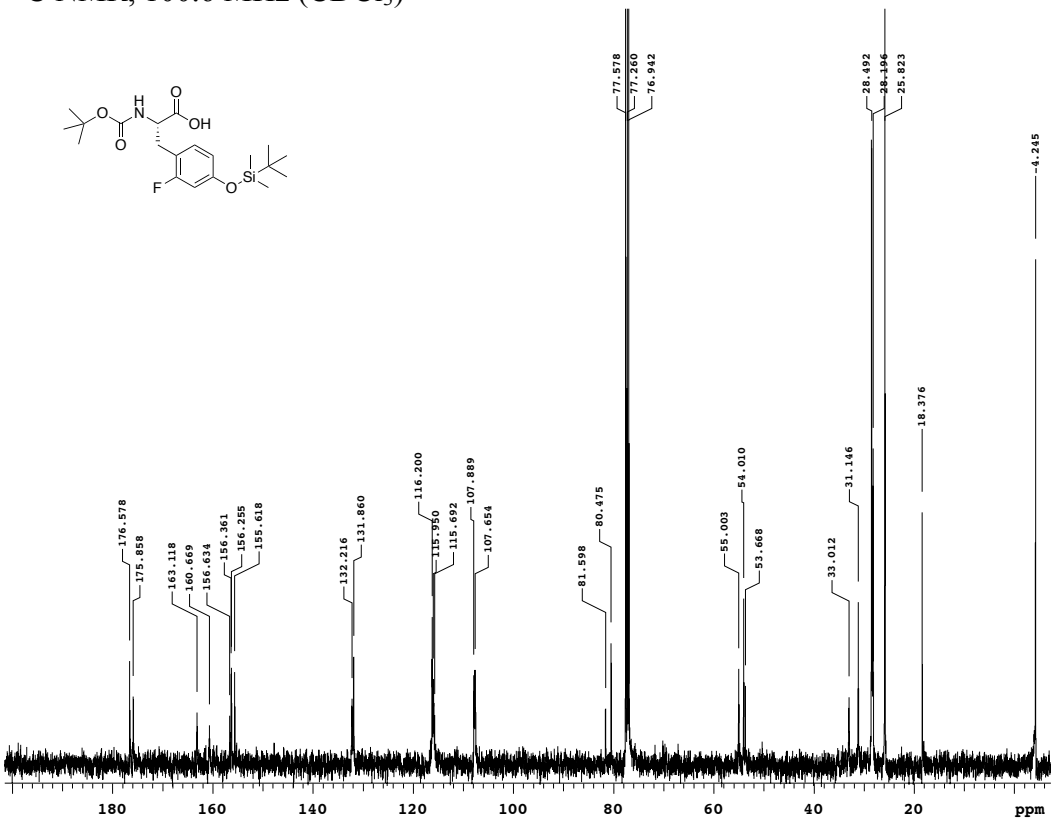

^{19}F NMR, 376.4 MHz ($CDCl_3$)

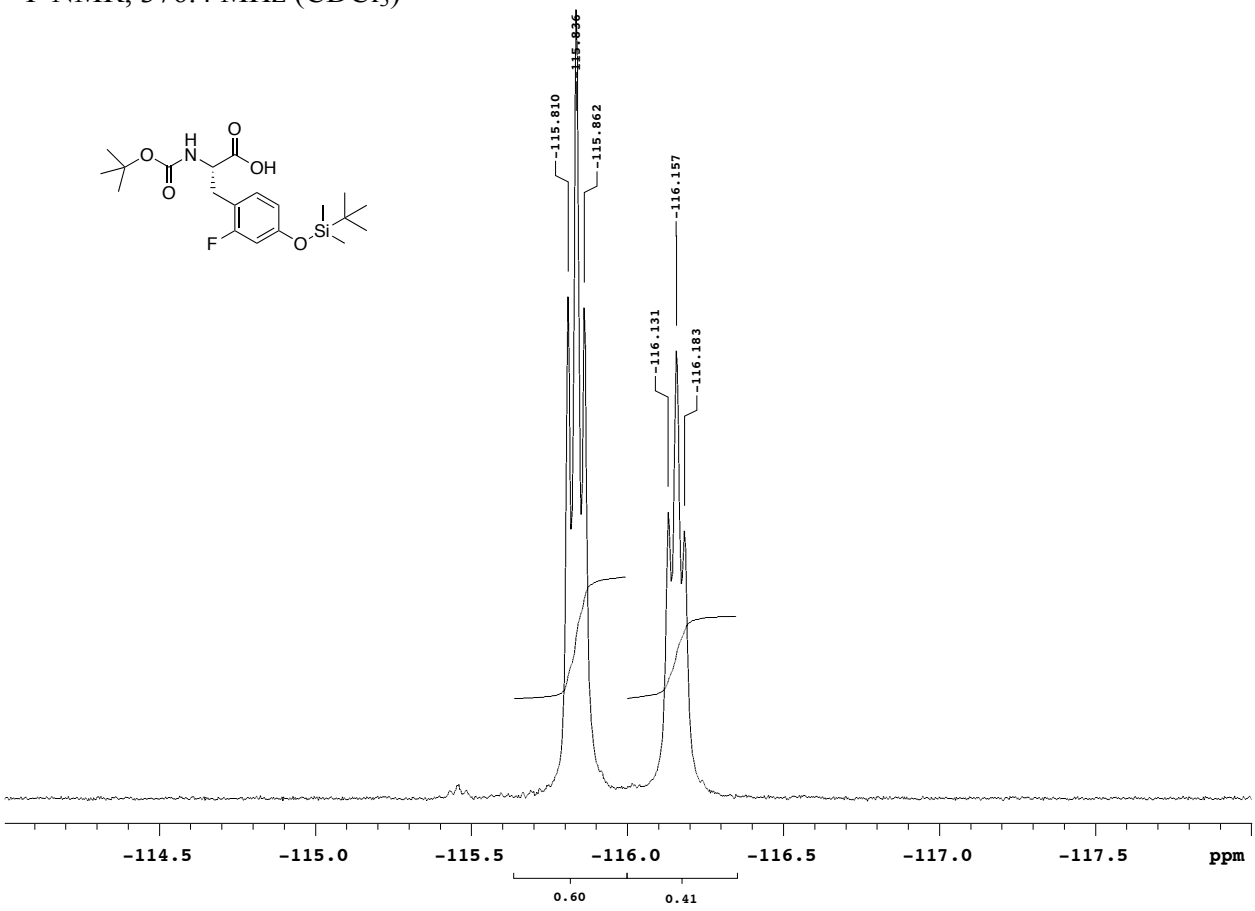

6. (*S*)-2-((*tert*-butoxycarbonyl)amino)-3-(4-((*tert*-butyldiphenylsilyl)oxy)-3-fluorophenyl)propanoic acid. ^{1}H NMR ($CDCl_3$); δ 9.14 (br s, 1 H), 7.70 (d, J = 7.5 Hz, 4 H), 7.43 (t, J = 7.5 Hz, 2 H), 7.36 (t, J = 7.5 Hz, 4 H), 6.88 (d, J = 11.0 Hz, 0.37 H), 6.83 (d, J = 11.0 Hz, 0.73 H), 6.57 (s, 0.77 H), 6.56 (s, 1.23 H), 6.35 (br s, 0.35 H), 4.88 (d, J = 7.9 Hz, 0.68 H), 4.50 (q, J = 5.97 Hz, 0.70 H), 4.30 (br s, 0.33 H), 2.90 (m, 2 H), 1.41 (s, 6.4 H), 1.31 (s, 3.1 H), 1.13 (s, 9 H). ^{13}C NMR ($CDCl_3$); δ 176.40, 176.01, 155.53, 154.53, 152.91, 142.66 (d, J = 11.8 Hz), 135.69, 132.79, 130.24, 129.60, 127.98, 125.08, 124.91, 121.63, 121.38, 117.45 (d, J = 20.3 Hz), 81.76, 80.59, 56.08, 54.38, 38.59, 37.11, 28.50, 28.26, 26.73. ^{19}F NMR ($CDCl_3$); -131.35 (dd, J = 10.96 Hz, 6.70 Hz, 0.65 F), -131.80 (dd, J = 10.96 Hz, 6.70 Hz). Calculated mass (M-H) = 536.23; found 536.42 (ESI-MS).

^{1}H NMR, 600 MHz ($CDCl_3$)

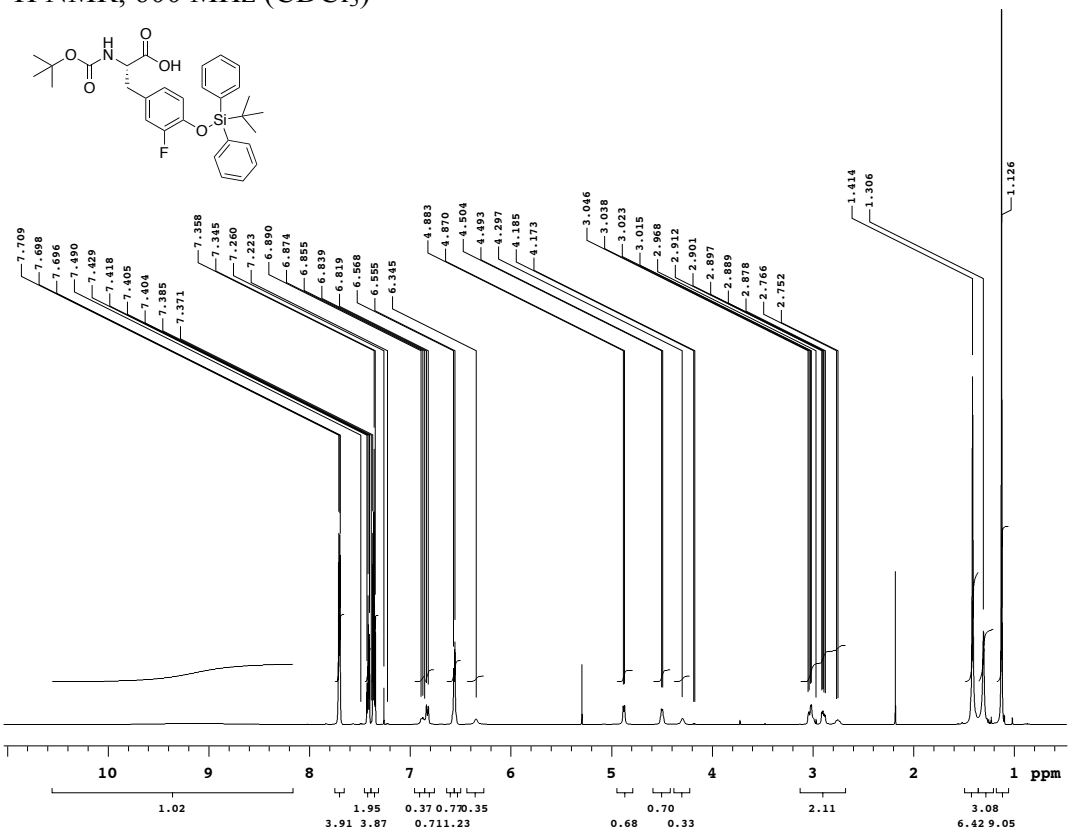

^{13}C NMR, 150.9 MHz ($CDCl_3$)

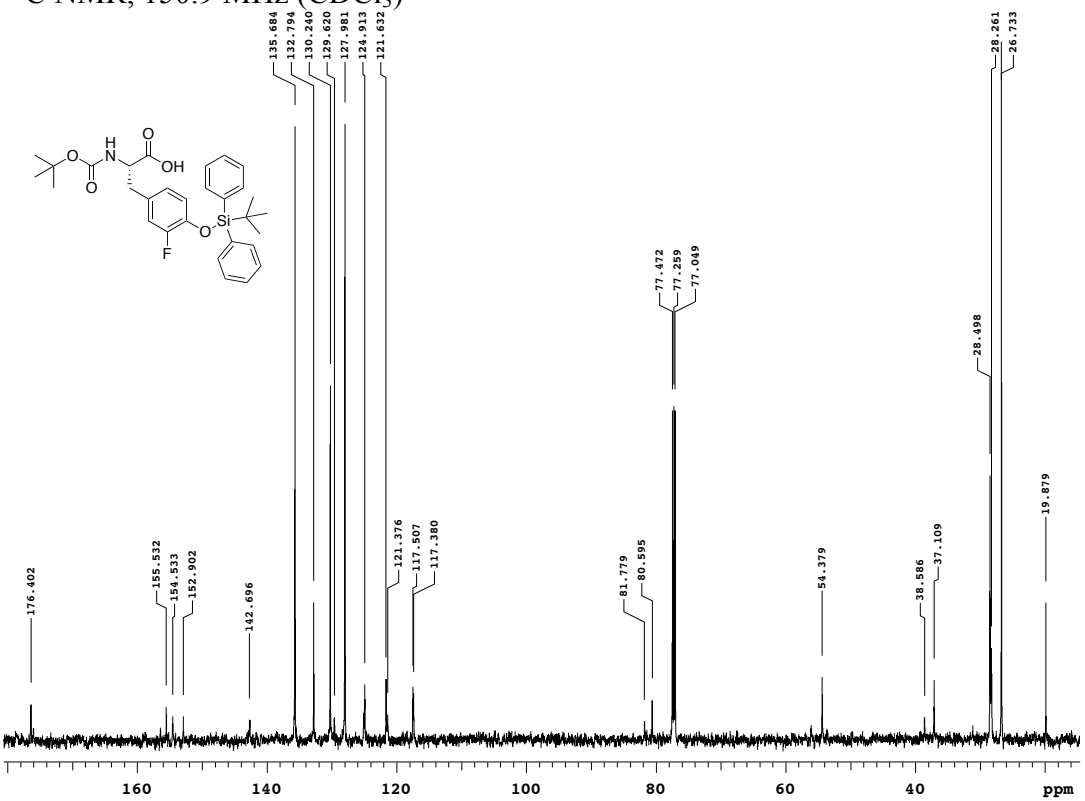

^{19}F NMR, 376.4 MHz ($CDCl_3$)

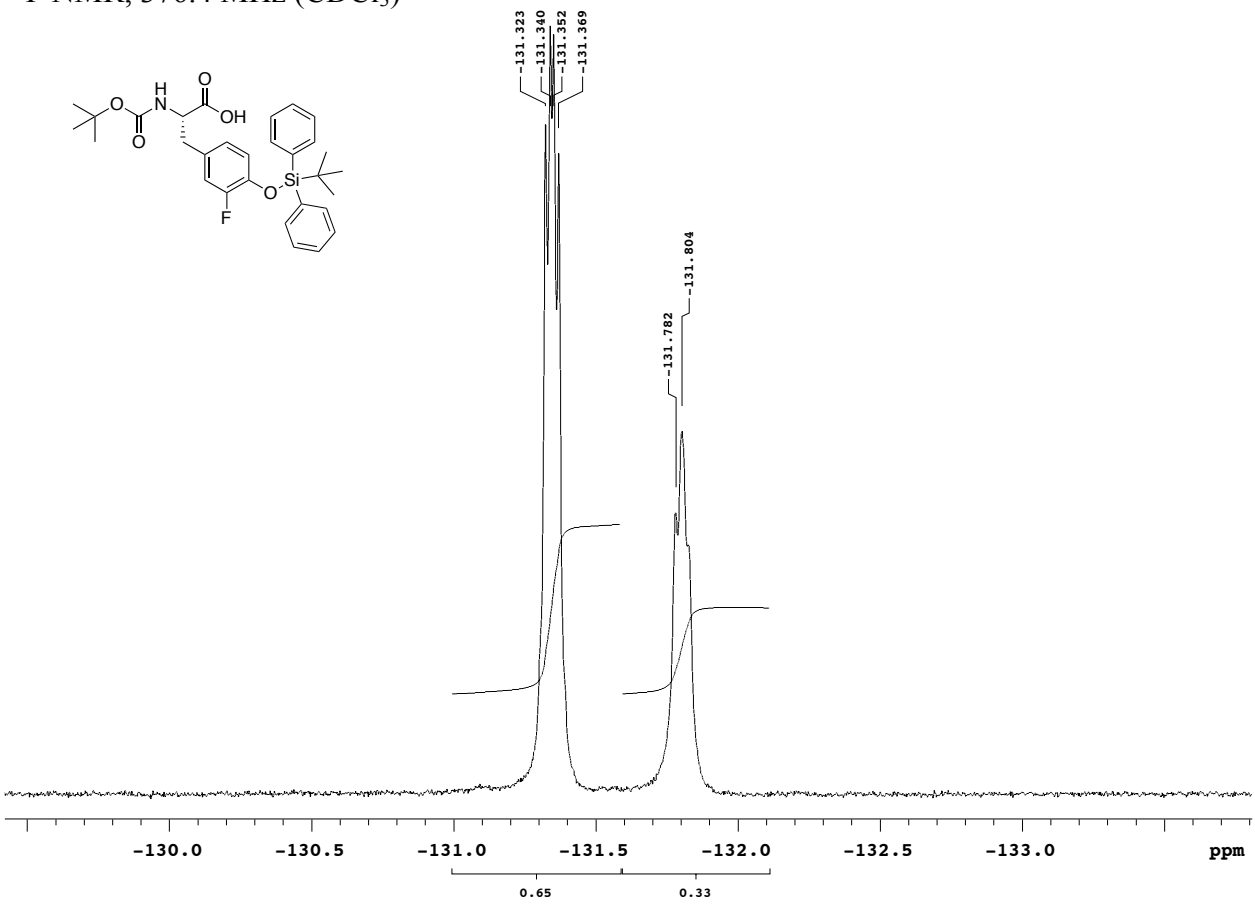

7. **(*S*)-2-((*tert*-butoxycarbonyl)amino)-3-(4-((*tert*-butyldiphenylsilyl)oxy)-2,6-difluorophenyl)propanoic acid.** ^{1}H NMR ($CDCl_3$); δ 10.55 (br s, 1 H), 7.68 (d, J = 7.0 Hz, 4 H), 7.42 (t, J = 7.0 Hz, 2 H), 7.36 (t, J = 7.0 Hz, 4 H), 6.72 (d, J = 8.5 Hz, 0.54 H), 6.29 (d, J = 8.9 Hz, 2 H), 5.07 (d, J = 8.5 Hz, 0.48 H), 4.51 (m, 0.49 H), 4.40 (m, 0.53 H), 3.10 (m, 1 H, 2.09 (m, 1 H), 1.36 (s, 4.5 H), 1.25 (s, 4.8 H), 1.09 (s, 9 H). ^{13}C NMR ($CDCl_3$); δ 176.26, 175.21, 163.93, 162.88 (dd, J = 23.8 Hz, 12.2 Hz), 161.24 (dd, J = 24.0 Hz, 12.6 Hz), 156.05 (q, J = 15.9 Hz), 156.61, 155.45, 135.57, 132.04 (m), 130.44, 128.15, 127.9, 105.73 (t, J = 21.1 Hz), 105.01 (t, J = 21.1 Hz), 103.53 (m), 81.49, 80.22, 54.17, 53.17, 37.11, 32.02, 31.02, 28.37, 28.07, 26.58, 25.34. ^{19}F NMR ($CDCl_3$); δ -113.91 (d, J = 9.1 Hz, 0.55 F), -113.98 (d, J = 9.1 Hz, 0.46 F). Calculated mass (M-H) = 554.23; found 554.30 (ESI-MS).

^{1}H NMR, 600 MHz ($CDCl_3$)

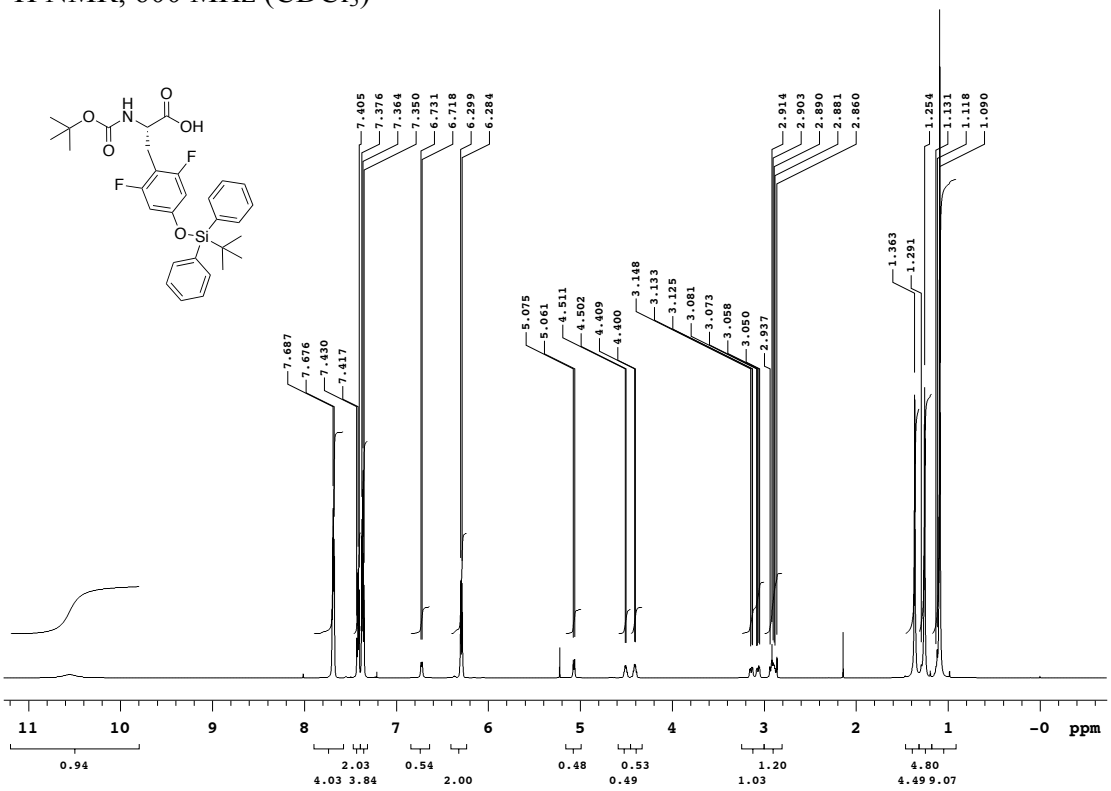

^{13}C NMR, 150.8 MHz ($CDCl_3$)

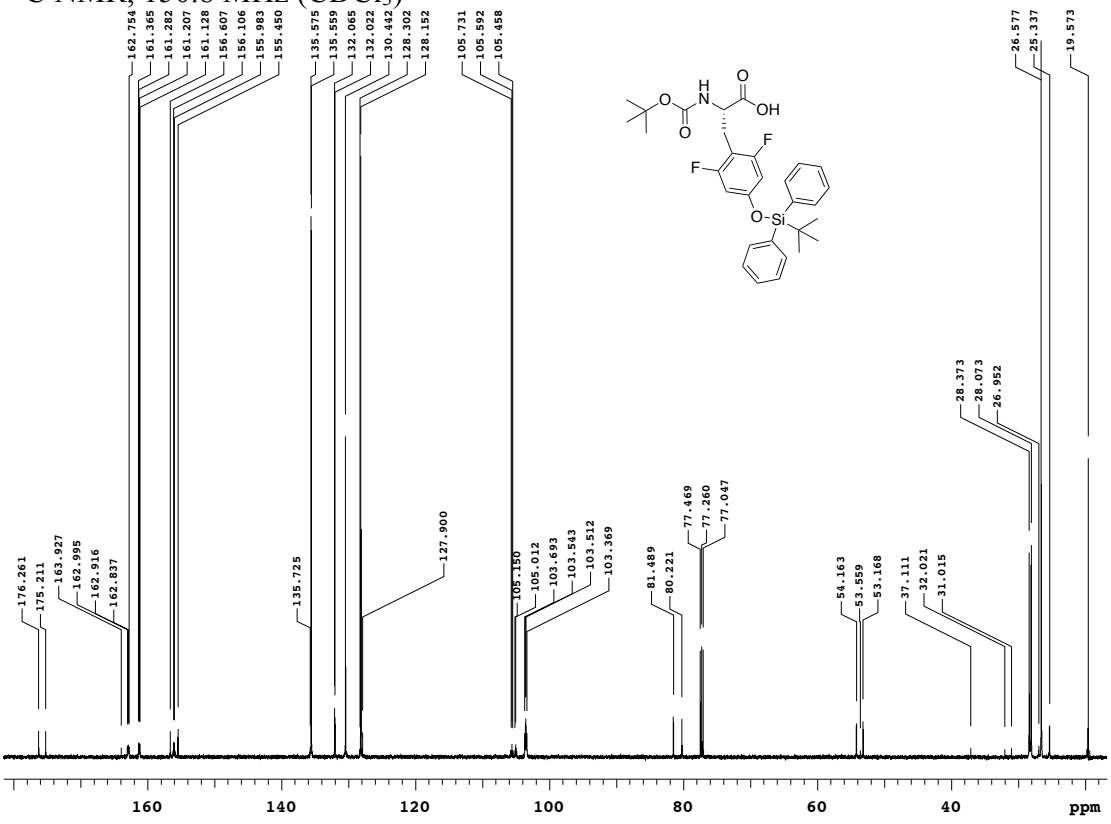

^{19}F NMR, 376.4 MHz ($CDCl_3$)

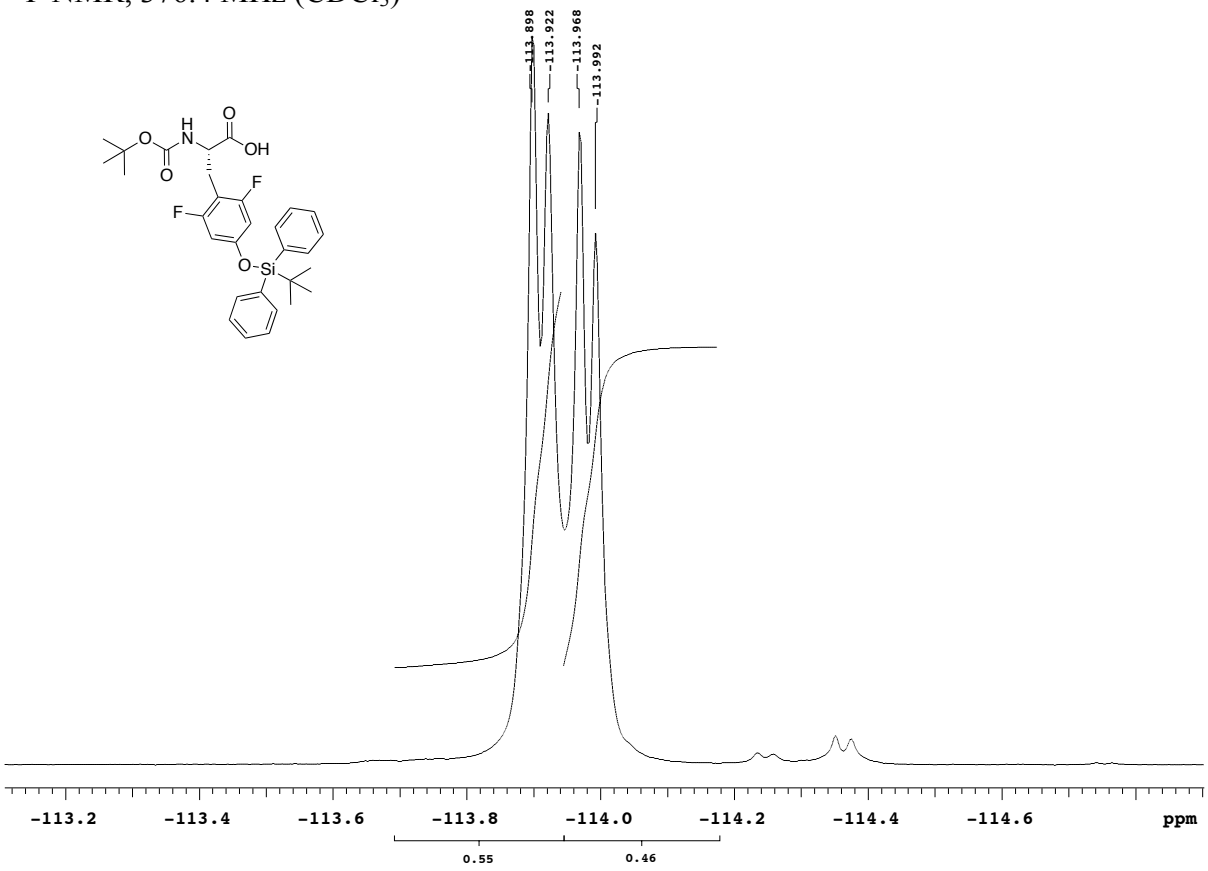

8. **(*S*)-2-((*tert*-butoxycarbonyl)amino)-3-(4-((*tert*-butyldiphenylsilyl)oxy)-3-chlorophenyl)propanoic acid.** ^{1}H NMR ($CDCl_3$); δ 7.71 (m, 4 H), 7.40 (m, 6 H), 7.21 (s, 0.3 H), 7.16 (s, 0.7 H), 6.62 (d, J = 8.6 Hz, 1 H), 6.42 (d, J = 8.6 Hz, 1 H), 6.17 (br s, 0.3 H), 4.91 (d, J = 8.0 Hz, 0.7 H), 4.49 (q, J = 6.6 Hz, 0.7 H), 4.29 (q, J = 6.6 Hz, 0.3 H), 2.92 (m, 2 H), 1.41 (s, 6.5 H), 1.30 (s, 2.5 H), 1.13 (s, 9 H). ^{13}C NMR ($CDCl_3$); δ 177.45, 176.56, 156.31, 155.48, 150.62, 135.69, 135.03, 132.52, 131.18, 130.30, 129.59, 128.28, 128.08, 125.08, 120.27, 120.08, 81.70, 80.55, 56.06, 54.38, 38.25, 36.94, 28.49, 28.26, 26.68, 21.00, 19.94. Calculated mass (E-H) = 552.21; found 552.14 (ESI-MS).

^{1}H NMR, 600 MHz ($CDCl_3$)

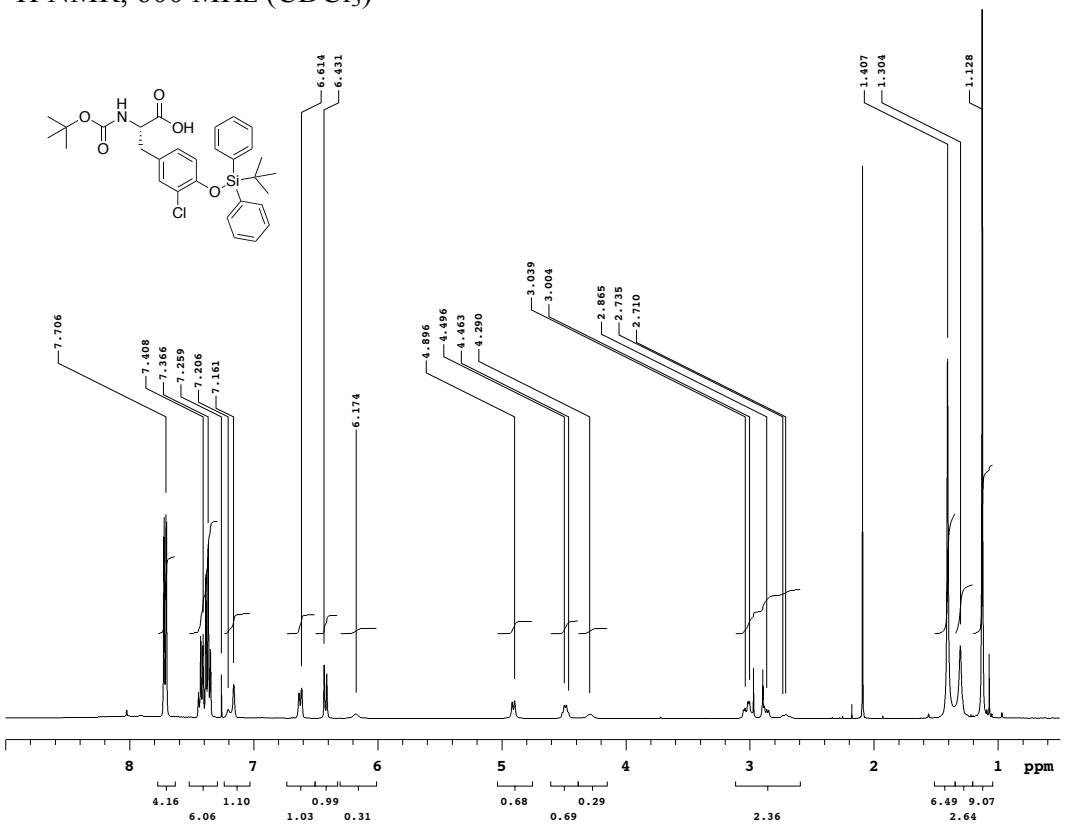

^{13}C NMR, 150.8 MHz ($CDCl_3$)